LUT UNIVERSITY
LUT School of Energy Systems
LUT Mechanical Engineering

Dezhi Jiang

SIMULATION TOOLS FOR RAILROAD DYNAMICS

28.11.2020

Examiners: Professor Aki Mikkola
D. Sc. (Tech.) Kimmo Kerkkänen

ABSTRACT

LUT University
LUT School of Energy Systems
LUT Mechanical Engineering

Dezhi Jiang

Simulation tools for railroad dynamics

Master's thesis

2020

50 pages, 43 figures, 5 tables and 1 appendix

Examiners: Professor Aki Mikkola
D. Sc. (Tech.) Kimmo Kerkkänen

Keywords: Railroad dynamic, Universal Mechanism, lookup table method, KEC method.

The objective of the work is to evaluate the accuracy of two methods which are implemented in MATLAB (by Xinxin Yu) against a commercial software in case of Manchester Benchmark parameters (Iwnick, 1998). Two methods and the software above are all simulation tools for railway dynamics. The methods are the lookup table method (Escalona and Aceituno, 2019) and knife-edge-equivalent contact constraint (KEC) method (Escalona et al., 2019). The method of evaluation is comparing the simulation results of above two methods with the results from commercial software, Universal Mechanism (UM).

Theoretical foundations for UM including information about wheel rail pair for this thesis, hunting, suspension systems, as well as cubic spline interpolation for profiles and irregularity are introduced. Integrators and contact models of UM, GENSYS and VI-Rail are investigated. Then a step-by-step example of building bogie with a primary suspension system in UM is shown.

Comparison results between above mentioned methods and UM are shown in Chapter 4. The first simulation is single wheelset forward motion on a tangent track with different speeds. Hunting frequency calculated by using Klingel's formula is the same as the frequency measured in simulation. During second set of simulation, the single wheelset travelled on a large radius curve and a small radius curve accordingly. The calculation result of the symmetry axis is the same as it measured from the result figure. Then the whole vehicle according to Manchester Benchmark standard (Iwnick, 1998) is applied. The whole vehicle is simulated on the small curve track. First travelled without irregularity, then with irregularities. The output results are the lateral displacements, and the yaw angles of each wheelset. Results from the lookup table method, the KEC method and UM agree well with each other. It can be concluded that lookup table method and the knife-edge-equivalent contact constraint method in case of Manchester Benchmark are verified against UM because they can get very close results with commercial software.

ACKNOWLEDGEMENTS

I would like to thank my supervisors Aki Mikkola and Kimmo Kerkkänen for their guidance for my thesis. I would also like to thank Xinxin Yu for her cooperation on the simulations. Thank Jussi Maksimainen at RAND Finland Oy, Volker Beuter at VI-grade, Ingemar Persson at AB DEsolver for providing knowledge about different commercial railway simulation software.

I have met some people who have deep friendship with me here in Lappeenranta during my studies. I would like to thank you for those unforgettable memories.

Finally, I would like to thank my parents for their support financially and companionships through internet.

TABLE OF CONTENTS

1 INTRODUCTION

Urbanization is making the scale of cities expending, the negative influence of environment such as air pollution, the reduction of open space, farmland, the diversity of species (Johnson, 2001). The need for transportation is growing among cities. Growth of motor vehicle ownership adds more stress to traffic. Meanwhile, building more and wider roads cannot solve the problem because road construction cannot follow the speed of vehicle growth. Local recreation areas which are good for the both mental and physical health of city residents are reduced (von Hertzen, Hanski, & Haahtela, 2011). Constructing underground and light rail is another solution. However, as underground and light rail need high investment and have a high volume of transportation, long construction cycle and complex technology. The underground and light rail are more suitable for big cities with good economy shape. Building trams is a good solution due to its less investment, low operating costs, safe and reliable rail transit mode. Trams can, improve road capacity and less pollution of a public transport system.

Railroad vehicles such as trams, underground and trains are extensively used methods for carrying people and goods. Due to rail transportation technology, modern trains can function in high speed with optimized costs and time. Railway transport also has lower carbon dioxide emission than airplane (www.dw.com, 2018). Airplane transports are restricted since COVID-19 outbreaks in 2020. Limited flights and high costs make airplane transport not the best option for transporting industries and medical supplies. Container trains transport has become the best option for Finnish companies and the volume of railway freight had already hit a high record before April (english.anhuinews.com). Besides cheaper than airfreight, the advantage of railway transport during the epidemic is that, transporting containers does not need additional personal. Unlike the shipping transport, ship crews need to obey quarantine regulations in destination cities, which increase the round-trip time. What is more, if one of the crew is infected in limited space such as ships, others are in high risk during the journey.

At the same time, safety, comfort level and low noise are still main issues. Derailment can be eliminated by identifying the causes of it. The comfort level and reduced noise can be achieved by limiting vibrations. Modern trains that have complex structure can be easier

simulated by modern computational dynamics. Dynamic simulation of railroad can help improve existing railroad vehicles. Figure 1 shows a tram in front of Helsinki Central Railway Station.

Figure 1. Tram in front of Helsinki Central Railway Station.

As the computer aided analysis is becoming an important method in design processes, simulations of electrical systems, hydraulic systems, robots, mechanisms, machines, and vehicles have been used widely. Unlimited numbers of measurable parameters can be measured by non-invasive methods. It is less time-consuming and cheap compare with experimental studies.

Computational dynamics provide tools for multi body system dynamic simulation. Usually there are various tools available for the simulation of a system. With the help of advanced computers with high calculating speed, analysing complex systems where there are lots of bodies and joints became possible. Conventional approached based on Lagrangian mechanics and Newtonian mechanics are converted into suitable forms for computers. (Shabana, 2009)

1.1 Objectives

This work comes from Smart tram project (www.vttresearch.com) with reference 6292/31/2018 and supervised by Xinxin Yu. The objective of the work is to evaluate the accuracy of the lookup table method (Escalona and Aceituno, 2019) and knife-edge-equivalent contact constraint (KEC) method (Escalona et al., 2019) which are implemented

in MATLAB (by Xinxin Yu) in case of Manchester Benchmark parameters (Iwnick, 1998). Two methods and the software mentioned above are all simulation tools for railway dynamics. The method of evaluation is comparing the simulation results of above 2 methods with the results from commercial software, Universal Mechanism (UM).

The evaluation process includes three sets of experiments: single wheelset forward motion on a tangent track with different speed (15 m/s, 25 m/s, and 45 m/s); single wheelset travelling on a large radius (R= 4545 m) curve and a small radius curve (R= 235 m) accordingly; the whole Manchester Benchmark vehicle travelling on a small curve track (R= 500 m) without and with irregularities successively. The hunting frequencies, symmetry axes, lateral displacements, yaw angles are compared during the verification.

1.2 Structure of the thesis

Background and advantage of the railway vehicle is introduced in Chapter 1. The need for transportation is growing with urbanization. Railway transport is quick, cheap, and time saving. Especially during COVID-19 outbreak, the railway transport of goods between countries is more popular. Then the objective of this work is listed.

Theoretical foundations for UM including the rail wheel pair, hunting, suspension systems, as well as cubic spline interpolation for profiles and irregularity are introduced in Chapter 2.

The function and theory (integrator and contact model) of UM, GENSYS and VI-Rail are introduced in Chapter 3. Then an example of building bogie with the primary suspension system in UM is followed.

Chapter 4 includes results comparison and analysis between UM and Lookup table. The important contact parameters and the irregularities of the rails are emphasized. Results from lookup table method, KEC method and UM agree well with each other.

Chapter 5 summaries the thesis and concludes that the lookup table and the knife-edge-equivalent contact constraint method are verified because they can get very close results with the commercial railway dynamic software Universal Mechanism.

2 THEORETICAL FOUNDATION

The simulation software used in this thesis is Universal Mechanism. The profiles of wheels and rails, the geometries of track centerlines, the bogies and vehicle, the suspension systems, the irregularities are built in UM. Theoretical foundations of above steps in UM are introduced in this chapter.

2.1 Wheel rail pair

For railway vehicles in general, the wheelset consists of two wheels and an axle. The wheels are cone shape in general. There are two different parts in detail: flange and tread. The shape of the wheel rail pair can be found in Figure 2. Above design gives wheelsets the ability of self-steering during the motion on rails. The motion of steering consists of yaw and roll rotation. During the rotations, the lateral positions of the wheelset vary. The steering process is called hunting. Ideal condition shown in Figure 3 (a) is that when the wheelset is traveling on rail, only tread part contact with rail. There is only normal contact force between wheel treads and rails. If the hunting oscillation is violent or the wheelset is passing small-radius curve, flange contact will occur as shown in Figure 3 (b). Besides normal contact force between wheel tread and rail, there is another contact force between the wheel flange and rail. There is a risk of derailment for the vehicle if the flange contact is violent. The default contact model in Universal Mechanism is FASTSIM.

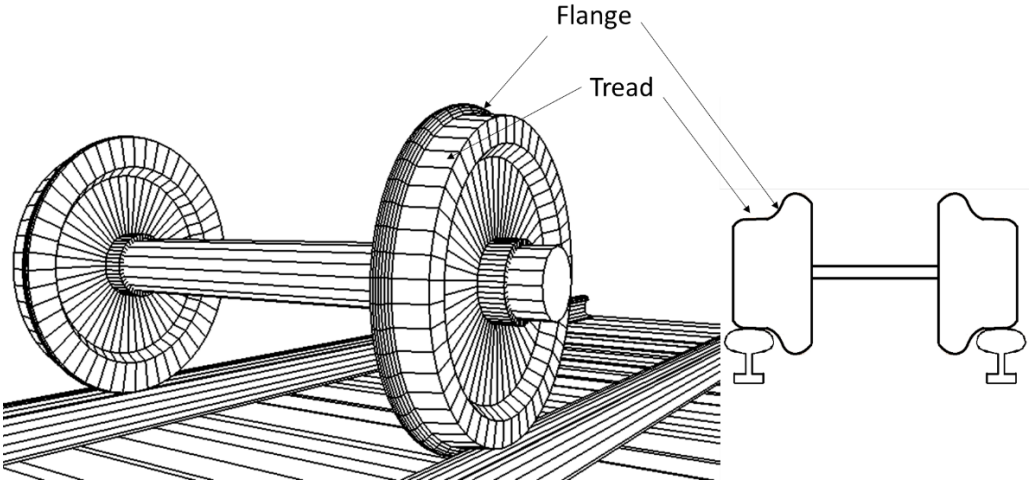

Figure 2. Schematic diagrams of wheel rail pair.

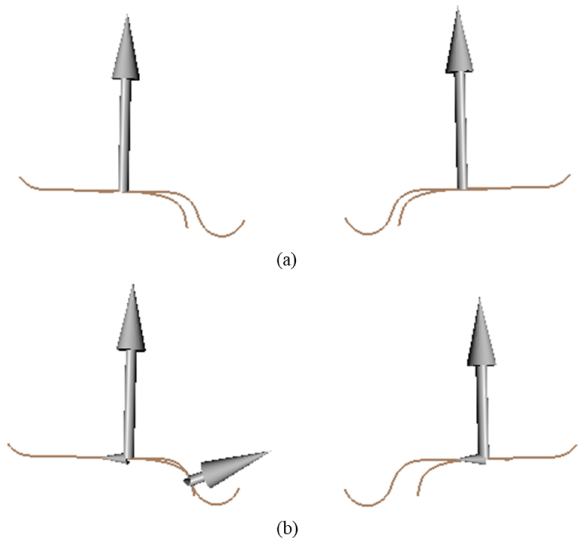

Figure 3. Tread contact (a) and flange contact (b) of wheel rail pair.

Evaluating the motion of the whole vehicle or vehicle parts are important in railway vehicle dynamics. There are 6 degrees of freedom for wheelset and rail relative motions (Pombo, et al., 2004). The type of the motions, as well as their description, symbol, and representation symbol in UM are listed in Table 1. Figure 4 shows the coordinates for one wheelset in UM.

Table 1. *Explanations of relative motions*

Motion type	Description	Symbol	Symbol in UM
Longitudinal	Forward translation	x	X1.1
Lateral	Translation in lateral direction	y	X1.2
Vertical	Translation in vertical direction	z	X1.3
Roll	Rotation about Y axis	φ	X1.6
Pitch	Rotation about X axis	χ	X1.5
Yaw	Rotation about Z axis	ψ	X1.4

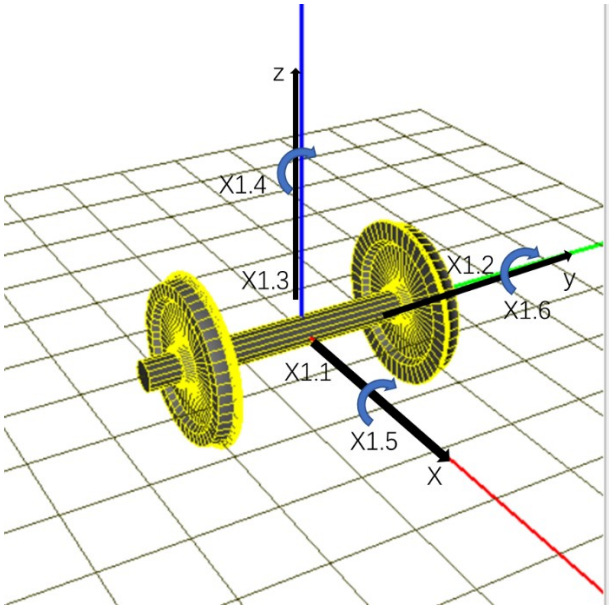

Figure 4. Wheelset and coordinates in UM Input.

2.2 Suspension system

The suspension systems in railway vehicles absorb vibrations which are harmful to vehicle elements during the journey. For example, hunting oscillation can lead the vibration of wheelset axle. If the vehicle travels under critical speed, the amplitude will gradually approach 0 because of the suspension system. In general, the suspension system consists of primary and secondary suspension. (Anon) (Continental-railway.com, 2020)

Primary suspension connects the wheelsets and bogie. During simulation for this thesis, as Figure 5 shows, there are 3 sets of springs (in longitudinal, lateral, and vertical direction) and 1 set of dampers (vertical direction) attached to wheelsets. With primary suspension, the bogie with wheelset can stably travel on track with irregularities.

Secondary suspension connects car body with bogie. For each bogie, there are 2 set of dampers (in lateral and vertical direction), 1 set of springs (in vertical direction) and a traction rod (in longitudinal direction). The function of secondary suspension is reducing the effect of track irregularity on the vehicle. Figure 6 shows the dimensions of the suspension system. Figure 7 shows the overall view of the suspension system with the whole vehicle.

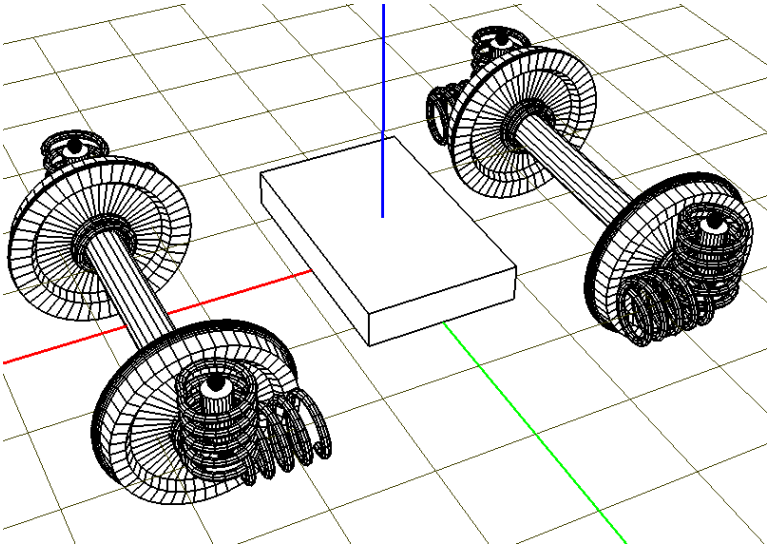

Figure 5. Primary suspension between bogie and wheelset.

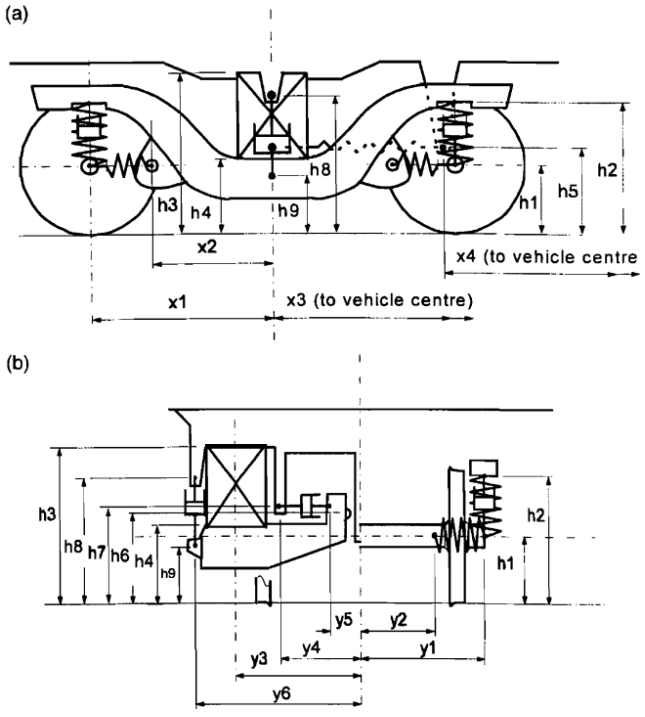

Figure 6. Dimensions of Manchester Benchmark vehicle suspension system (Iwnick, 1998).

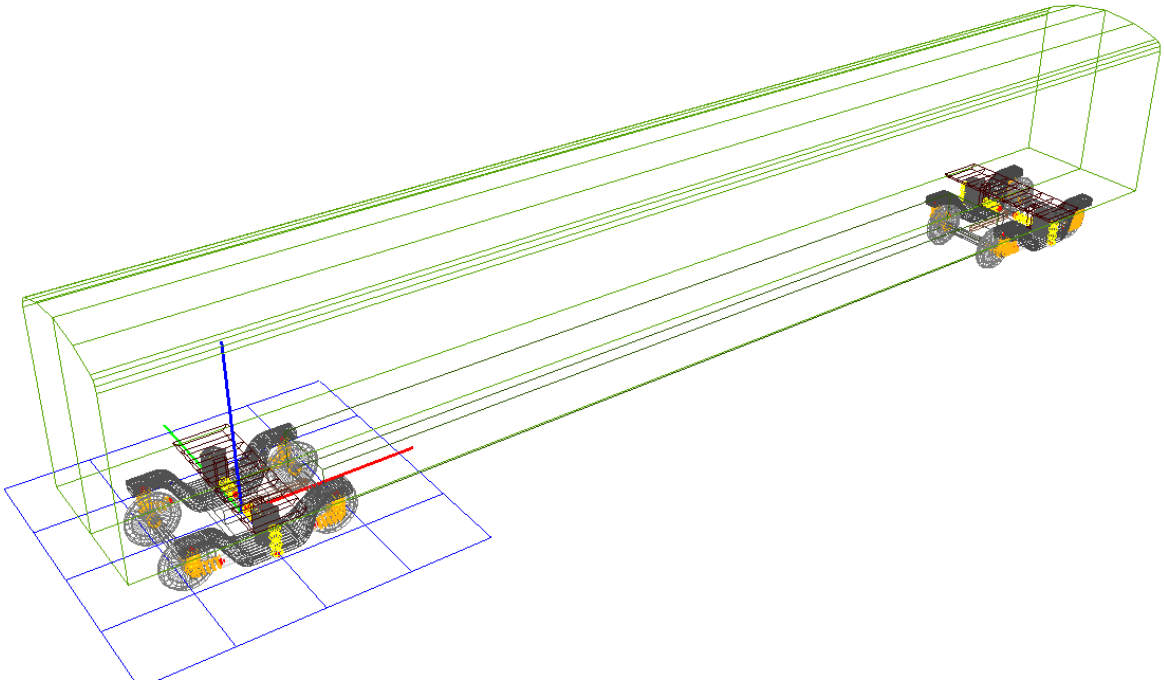

Figure 7. Overall view of suspension system with the whole vehicle.

2.3 Hunting and critical speed

The hunting oscillation of a railway vehicle is a phenomenon that wheelset have an 'S' shape movement from top view when the vehicle moving forward. When wheelset is not centered on the track, there will be a difference of effective diameter (R_0) between two wheels because of cone tread. The condition above will lead to a lateral oscillation together with yaw rotation named hunting oscillation, where the system is hunting for equilibrium. Hunting can be resulted by high conicity. Critical hunting has negative influence on characteristics: decrease the comfort level, make the train more easily to derailment and harmful to the track. (Shevtsov, et al., 2005) (Sun, et al., 2019)

Common understanding of critical speed expects hunting oscillation. The oscillation increases with increasing speed. For soft subgrade railways, if trains travel near or faster than the Rayleigh wave velocity of subgrade soil, the speed is critical speed. (Gao, et al., 2017) In this thesis, critical speed is measured as speed when suspension systems can no longer reduce hunting phenomenon. Hunting frequency has a huge effect on wheelset hunting. The forward speed has positive correlation with hunting frequency. (Sun, et al., 2019)

2.4 Interpolation methods for cubic spline

The wheel and rail profiles, centerline of general tracks, and track irregularities are all defined by a set of points in simulation for this thesis. Cubic splines connect every two neighboring points. So, the first and second derivatives of every point in the spline segment can be calculated. The cubic spline is defined as (Barsky, 2013):

$$g(u) = a_3u^3 + a_2u^2 + a_1u + a_0 \tag{1}$$

where $g(u)$ is the point on the spline, u is variable, coefficients a_i needed to be calculated. Presume that there are 2 points defined by user: (0,1) and (1,2). The points are substituted into equation (1). The equation and its first derivative are:

$$\begin{cases} g(1) = a_3 + a_2 + a_1 + a_0 \\ g'(1) = 3a_3 + 2a_2 + a_1 \\ g(2) = 8a_3 + 4a_2 + 2a_1 + a_0 \\ g'(2) = 12a_3 + 4a_2 + a_1 \end{cases} \tag{2}$$

as there are 4 unknowns and 4 equations. Coefficients a_i are solvable. The spline can be defined.

3 SOFTWARE TOOLS FOR RAILROAD DYNAMIC

Some well know commercial simulation software of railway dynamic are VI-Rail, GENSYS, SIMPACK, VAMPIRE (Pombo, et al., 2004). Integrators and contact models of GENSYS, VI-Rail and UM are counted by email interview and documentation reading.

Universal Mechanism (UM) is a multi-body system program package, which is for both planar and spatial mechanical systems. The application fields of UM are, for example, automotive, rail vehicles, flexible bodies, trains, tracked vehicles. (www.universalmechanism.com)

3.1 Integrators and contact model among commercial software

Originally, VI-Rail was implanted by MDI company as ADAMS/Rail. The name of the software became to VI-Rail after MSC company acquired MDI company. VI-GRADE was founded by former employees of MDI company so there is no change of developers. VI-Rail and ADAMS/Rail are technically the same. (Volker, 2020)

As of above reason, all integrators in Adams solvers are also available in VI-Rail. For example, GSTIFF, WSTIFF, HASTIFF, HHT and NEWMARK with different formulations and settings. The default integrator of VI-Rail is GSTIFF. GSTIFF is also recommended by the official documentation of VI-Rail.

VI-Rail uses contact implementation by W. Kik. Modified FASTSIM or the Polach method can be selected for the calculation of creep forces. Serval wheel rail elements available in VI-Rail are listed below (Volker 2020):

- Quasi-linear element type allows user to analyze the effects of parameters separately from defined rail and wheel profiles. The parameters include conicity, the contact angle, and roll angle. The vehicle stability can be learnt by using Quasi-linear element type.
- Element type with pre-calculated kinematic table uses an ellipse to approximate contact patch. This type is based in kinematics on defined rail and wheel profiles. A

constant value is used for the stiffness. There is one contact patch per interconnection only.

- Wheel rail interconnection element uses Boussinesk formulation to model non-elliptical contact patches and contact stiffness. The number of contact patches in one interconnection is not restricted. This element is the most general element among these three.

GENSYS does not recommend using high order integration methods to do railway vehicles dynamic simulations. It is because the flange contact between rail and wheel is highly non-linear. A method with few steps does not try to linearize the problem. It is more suitable for capturing the short duration of force peak. Different integration methods with their codes in GENSYS are listed in Table 2 below (Ingemar, 2020) :

Table 2. *Integration methods in GENSYS (www.gensys.se, modified).*

Code name	Explanation of the code
e1	Euler forward.
mp2	The midpoint method.
runge_kutta	The four step Runge-Kutta method.
heun	The two step Runge-Kutta method.
heun_u	The two step Runge-Kutta method with step size control.
heun_c	The two step Runge-Kutta method with step size control, may have backsteps.
heun_d	The faster execution of heun_c.
heun2impl	The implicit Heun's method.
dopri5	The explicit Runge-Kutta.
radau5	The implicit Runge-Kutta method of order 5.
odassl	The implicit DAE-solver.

There are many contact models available in GENSYS package. The full version can be found in Appendix 1. Three of the contact models that based on FASTSIM code and their code name are listed in Table 3 below:

Table 3. *Contact models related with FASTSIM in GENSYS (www.gensys.se, modified).*

Code name	Explanation of the code
creep_fasim_1	Rolling contact. Using linear spring and Kalker's fasim routine for normal contact and tangential contact accordingly.
creep_fasim_2	Similar to fasim_1, with different creepages formulas.
creep_fasim_4	Similar to fasim_1, but the wheel and rail profiles are used directly.

In addition, using "func wr_coupl_XXX" command in GENSYS can create both wheel/rail coupling and massless rail with stiffnesses and dampers under the rail. The advantage of this command is that the simulation runs faster with massless rails.

3.2 Integrators and contact model in Universal Mechanism

Various integration methods are available in UM. DAE (ordinary differential-algebraic) equations are for objects with closed kinematical loops. Integration methods below are for both DAR and ODE (ordinary differential equations) (UM Simulation Program User's manual 2018):

- **BDF**: Backward Differentiation Formula. This is an explicit prediction-evaluation-correction solver. Order is up to fifth. The step size and order may vary. BDF is for non-stiff equations only.
- **ABM**: Adams-Bashfort-Moulton method. This is explicit prediction-evaluation-correction-evaluation solver. Order is up to eleventh. Step size and order may vary. ABM is for non-stiff equations only.
- **PARK**: PARK is a second order implicit solver. The step size may vary. PARK is for stiff ODE and DAE.
- **GEAR 2**: GEAR 2 is a second order implicit method. The step size may vary.
- **RK4**: RK4 is the 4th order Runge-Kutta method. The step size is constant. RK4 is not suitable for DAE.
- **Park parallel**: Park parallel is finite-difference methods based on PARK. Equations of motion are generated by special methods. The Park parallel method utilizes multi-core processors to parallel computations. The Park parallel is more efficient than PARK.

3.3 Wheelset parameter

Figure 8 shows the geometry of the wheelset. Distance between wheelset center and wheel center, which is called 'Semibase' in UM, is $L = 0.7515$ m. Running circle radius $R_0 = 0.457$ m, Which is the distance between ideal contact point on tread and the center line of wheelset. Conicity alpha $\alpha = 0.025$ rad. Other parameters are listed in Table 4.

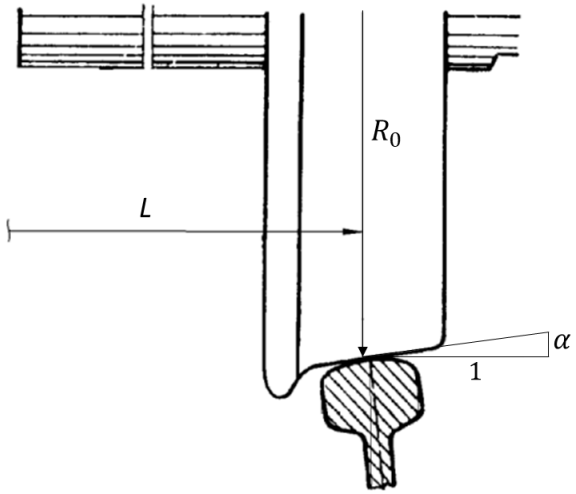

Figure 8. Wheelset geometry (Simulation of Rail Vehicle Dynamics User's manual, modified).

Table 4. *Wheelset parameter.*

Parameters	Model
Wheelset mass (kg)	1568
Wheelset inertia I_{xx} I_{yy} I_{zz} I_x^{wh} I_y^{wh} I_z^{wh} (kgm^2)	656, 168, 656
Running circle radius (m)	0.457
Semi base (m)	0.7515
Hertzian stiffness ($\mathrm{kN/m}^{1.5}$)	1×10^7
Damping parameter (kN/m/s)	1×10^5
Inclination angle (rad)	0.025

3.4 Creating a wheelset in UM input

Figure 4 in Chapter 2 showed the wheelset and coordinates in UM input. Parameters of wheelset and wheelset inertia can be modified under ‘general’ and ‘identifiers’ tab. The model needs to be saved in order to start simulation in UM Simulation software.

Path below shows the instruction of creating a wheelset:

- UM Input main menu > file > new object > subsystems > add new element > type: wheelset

Figure 9 shows setting the initial condition of wheelset. As mentioned before in Chapter 2, the 1.2 means the lateral position of wheelset 1. There are also +2 mm in lateral directions for every wheelset, bogie, and the car in later simulation. The path below shows the instruction of setting initial condition:

- UM simulation main menu > analysis > simulation > initial conditions > coordinates

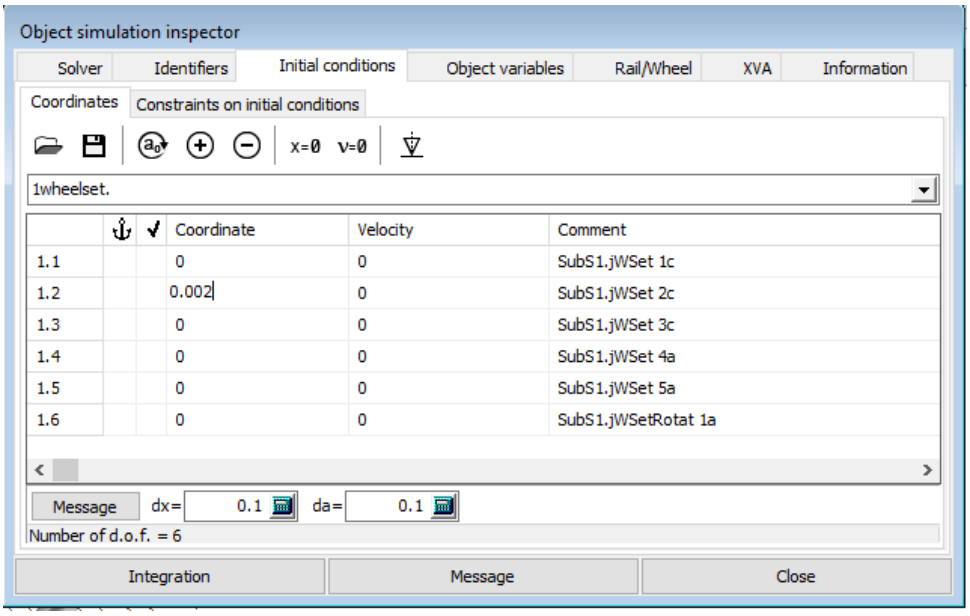

Figure 9. Setting initial conditions.

3.5 Wheel and rail profile

After wheelset is built and saved in UM input, simulation shall be started by ‘Run UM Simulation program’ function. Next step is setting wheel and rail profiles. Through the simulation inspector, ready wheel and rail profiles can be loaded. UM also allows editing

rail and wheel profiles by users. Path below shows the instruction of creating wheel and rail profile:

- UM Input main menu > tools > railway wheel and rail profile editor

Wheel and rail profiles are constructed using a set of nodal points. Spline interpolation is used to parameterize the profile. Point list consisted by two columns is pasted into the railway wheel and rail profile editor. The order of the list is ascending order with X axis. The unit is in millimeter. Figure 10 and Figure 11 shows the profiles of the right wheel and the right rail accordingly. The right wheel and right rail are the mirror of the left wheel and the left rail accordingly. Right wheel and rail profiles are enough to assign both rails and wheels.

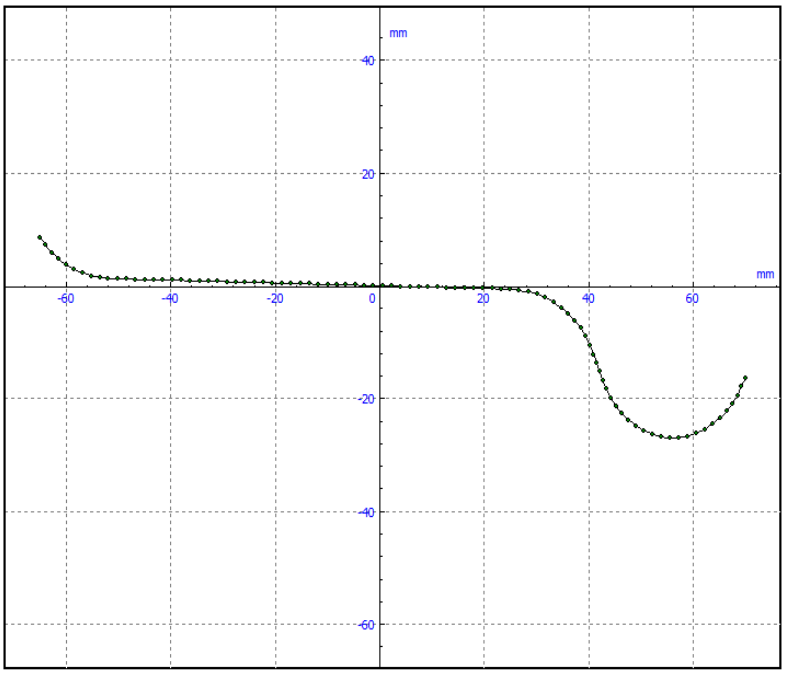

Figure 10. Right wheel profile built by points.

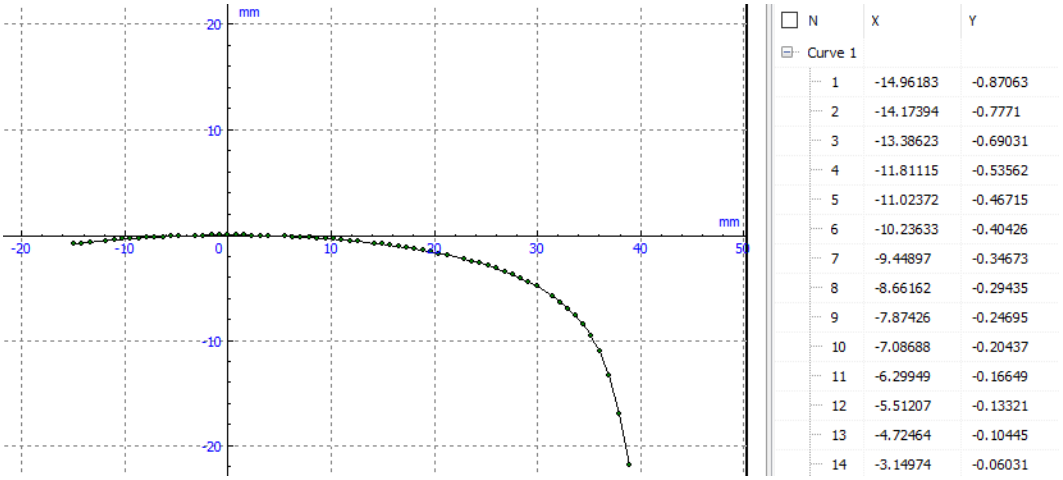

Figure 11. Right rail profile built by points.

Figure 12 shows the analysis of the right wheel and right rail profile. The type of contact is 2-point contact. The figure shows tread contact. In case of hunting motion, flange contact will appear.

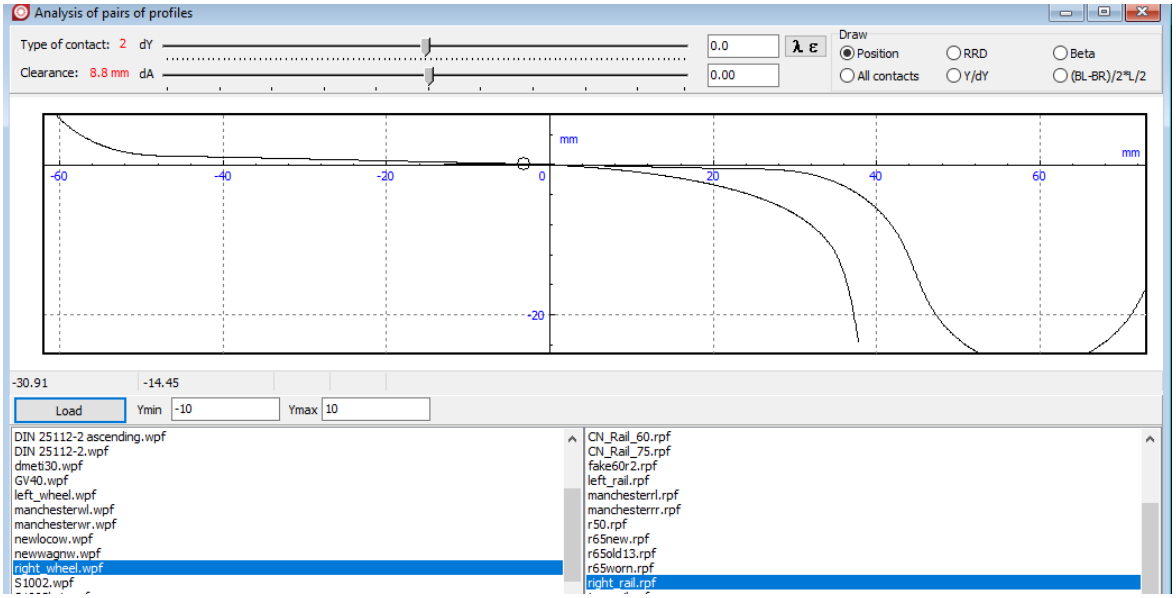

Figure 12. Analysis of right wheel and rail profile.

3.6 Track macro geometry

Track macro geometry can be defined both by various sections (including tangent sections, curve sections, switch sections) and pointwise curves. In this thesis, pointwise curves are used to describe track macro geometry. Figure 13 shows the horizontal track profile in UM

track macrogeometry editor. The vertical macro geometry is tangential. The path below shows the instruction of adding pointwise curve:

- UM Simulation main menu > tools > macrogeometry editor > railway or monorail track > add section > add pointwise curve

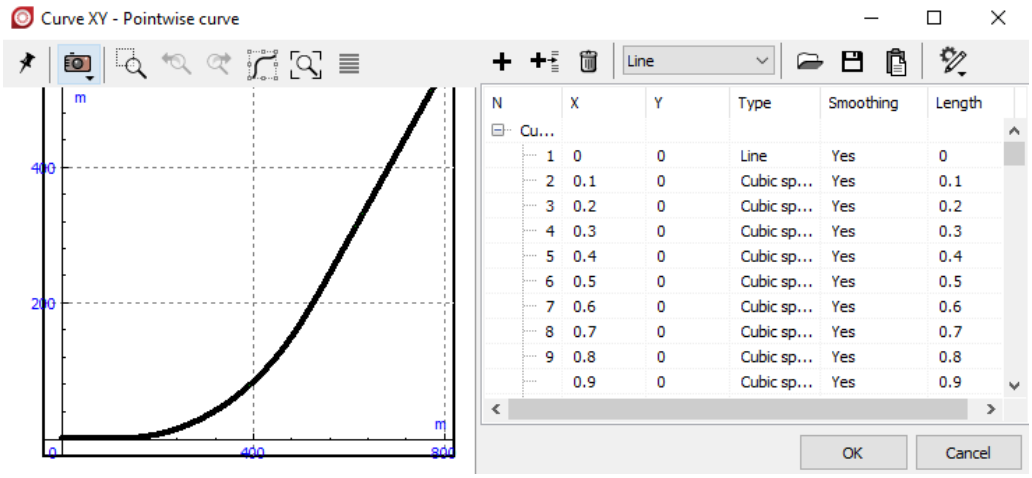

Figure 13. Horizontal track profile in the track macro geometry editor.

3.7 Simulation of one wheelset forward motion

Simulations of one wheelset motion are done under different speed and track type. On tangent tack, speeds of 15 m/s, 25 m/s, and 45 m/s are tested. The initial speed is constant applied on wheelset, if there is a bogie or a car in the simulation, it should be applied on the element which with the highest mass. Speed of 20 m/s is used in a steady curving large radius curve (R=4545 m) and small radius curve (R=235 m). Paths below show the instructions of initial speed, speed type, applying macro geometry, applying irregularities, applying wheel and rail profiles accordingly:

- UM Simulation main menu > Analysis > Simulation > Identifiers > List of identifiers > Whole list > v0
- UM Simulation main menu > Analysis > Simulation > Rail/Wheel > Speed > Mode of longitudinal motion > Neutral
- UM Simulation main menu > Analysis > Simulation > Rail/Wheel > Track > Macrogeometry > Track type > From file
- UM Simulation main menu > Analysis > Simulation > Rail/Wheel > Track > Irregularities

- UM Simulation main menu > Analysis > Simulation > Rail/Wheel > Wheels > Profiles
- UM Simulation main menu > Analysis > Simulation > Rail/Wheel > Rails > Profiles

Figure 14 shows setting of vehicle initial speed under identifiers tab in the object simulation inspector. Figure 10 shows the initial speed is set as constant and applied on the single wheelset. The speed should be applied to the bogie or the vehicle car if the testing subject is bogie or the whole vehicle accordingly. As it showed in Figure 16, mode of creep force is set as FASTSIM, Young's modulus is set as 2.1×10^{11}, Poisson ratio is set as 0.3.

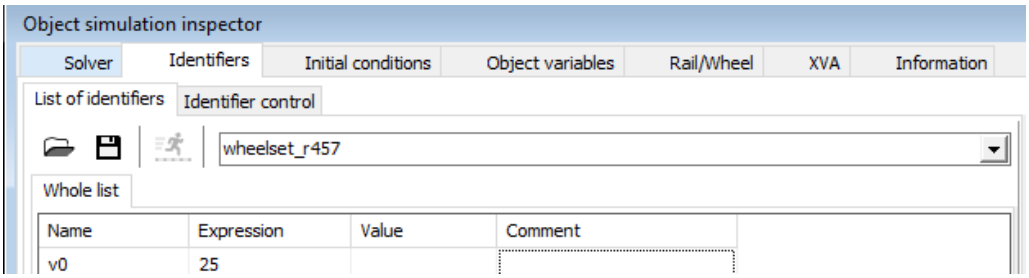

Figure 14. Setting of initial speed.

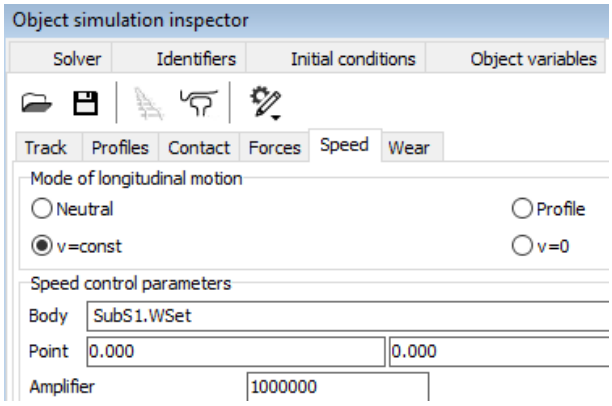

Figure 15. Setting of speed type.

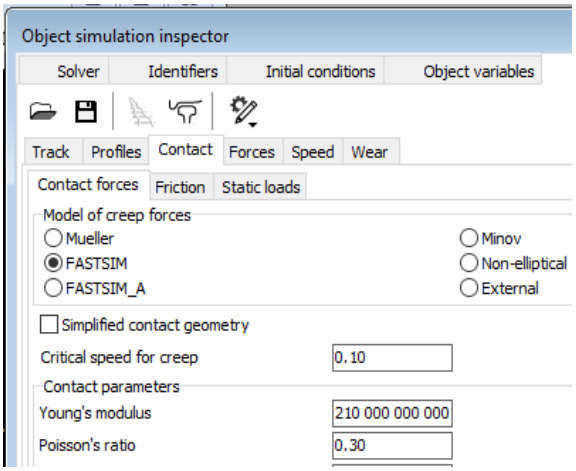

Figure 16. Settings of contact force.

3.8 Output numerical results

Desired variables can be chosen in ‘wizard of variables’ under ‘tool menu’. The lateral displacement of wheelset is considered as important output in this simulation. Figure 17 shows variables selected from the wizard of variables in plots. As shown in Figure 18, because lateral displacement is respect to the local coordinate of wheelset, it should be chosen under ‘Track Coordinate System’ in ‘Wizard of Variables’. The variable can be added into the container by double clicking. Variables for the yaw angles of wheelsets and positions alone tracks are under ‘Rail/Wheel’ tab. Results can be plotted into ‘Graphical window’ under ‘tool’ menu. Paths below show the instructions of graphical window, the wizard of variables, setting of lateral displacement and yaw angle, position along track accordingly:

- UM Simulation main menu > Tools > Graphical window
- UM Simulation main menu > Wizard of variables > Track coordinate system > WSet > Type > Coordinate > Component > Y
- UM Simulation main menu > Wizard of variables > Wheelsets > WSet1 > yaw
- UM Simulation main menu > Wizard of variables > Wheelsets > WSet1 > Position

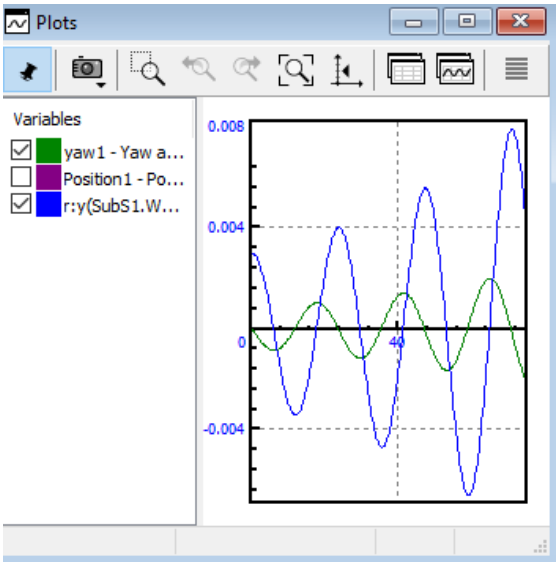

Figure 17. Plotting variable.

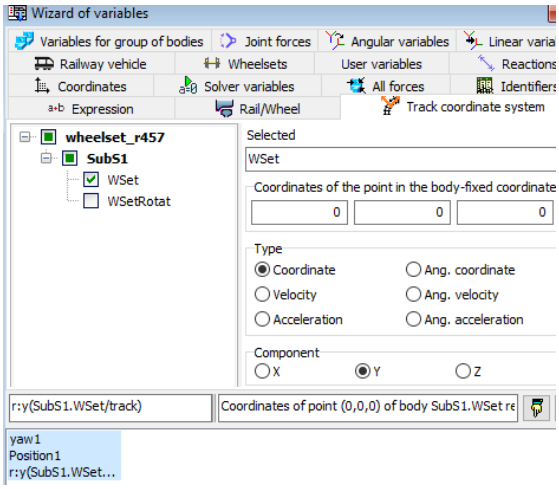

Figure 18. Setting variable for lateral displacement.

3.9 Example of creating one bogie with primary suspension

As Figure 5 in Chapter 2 shows, two wheelsets are suspended with a bogie (replaced by a box) by springs and dampers. The box and four set of springs with dampers are set as images in UM input, which means shapes have no influence on dynamic.

3.9.1 Creating wheelset

To create a new object file and wheelset, instructions below shall be followed:

1. UM Input main menu > File > New object

2. Object > Subsystems > Add new element > Type: Wheelset > Type of wheelset > Standard (Figure 19)
3. Object > Subsystems > Name

   Name of the wheelset can be changed to WSet1.
4. Object > Subsystems > Position > x1

   Enter the position value x1 for the wheelset. Then add identifier $x1 = 1.28$ according to Manchester Benchmarks for Rail Vehicle Simulation (Iwnick, 1998) (Figure 19)
5. Object > Subsystems > WSet1 > general and identifier

   Enter $R = 0.457$ m as radius of the wheelset, $L = 0.7515$ m as semibase. Enter the mass $mwset = 1813$ kg, moments of inertia $ixwset = 1120$ kgm^2, $iywset = 112$ kgm^2. (Figure 20)
6. Object > Subsystems > WSet1 (right click) > copy element

   After copying the wheelset, rename it as WSet2. Change the position of WSet2 to -x1. Same paths are used from above.

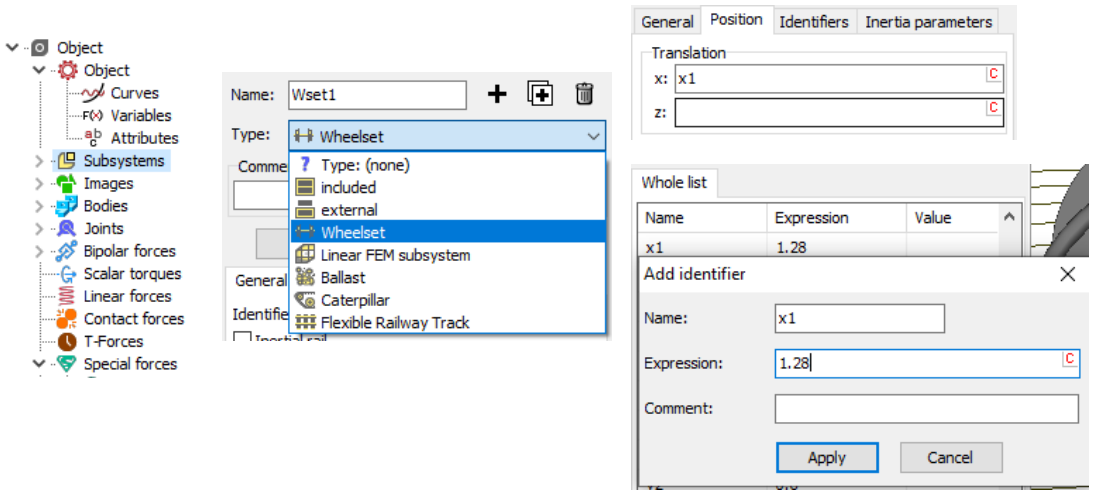

Figure 19. Adding a wheelset into subsystem.

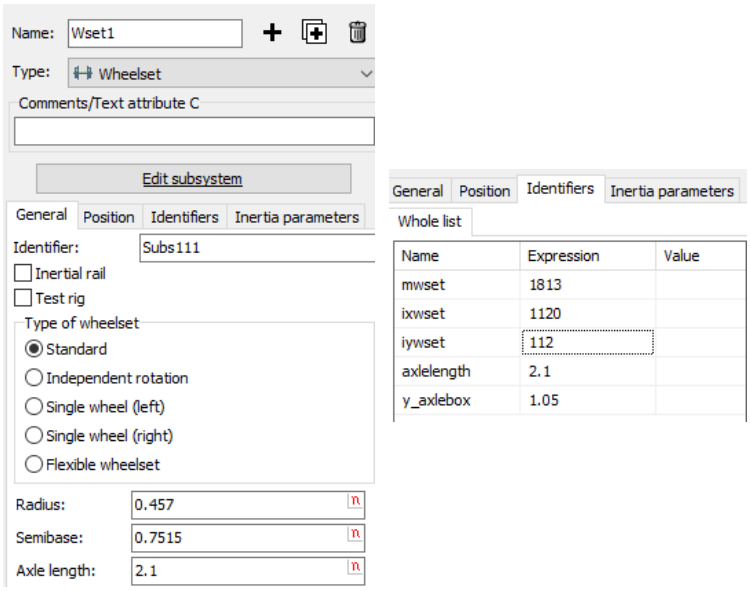

Figure 20. Mass and inertia parameter of wheelset.

3.9.2 Creating spring and damper as image

Spring and damper shape images are loaded to represent the spring and damper force of primary suspension for later use. Paths below are followed:

1. Object > Images > Add graphic object > Description > Type: Spring
   Rename the spring as 'SpringGO' to represent the spring for later use. The GO image of spring is created and shown in Figure 21.
2. Tool panel > Edit > Read from file> C:\Users\Public\Documents\UM Software Lab\Universal Mechanism\8\rw\Images\ > Damper

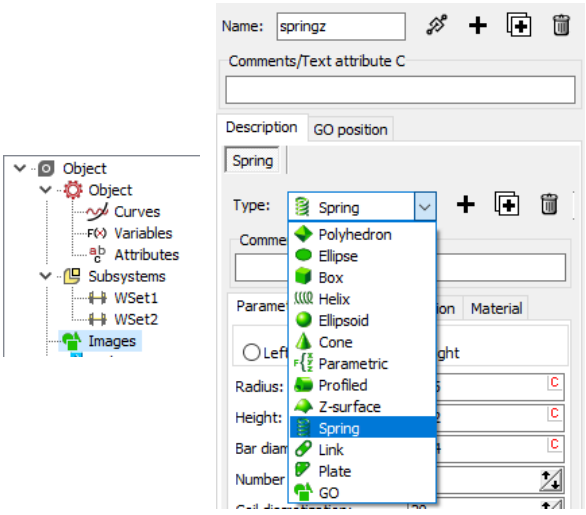

Figure 21. Adding image of spring.

3.9.3 Creating bogie

The bogie is created as an image, added to body so that it can react with primary suspensions. Paths below are followed:

1. Object > Images > Add graphic object > Description > Type: Box
   The same instructions are followed in creating spring as an image section. Rename the box as bogie. The image of bogie and its parameter is shown in Figure 22.
2. Object > Images > Add graphic object > Description > Parameter
   Parameters of the box are set and shown in Figure 22 referencing Manchester Benchmark.
3. Object > Bodies > Add new element > Parameter > Image > Bogie
   The image of bogie is added into body and shown in Figure 23 (a). Then mass and inertia parameter are set according Manchester Benchmark.
4. Object > Bodies > Parameter > Go to element > Create joint > 6. d. o. f.
   6 degrees of freedom is set as joint type and shown in Figure 23 (b). The degrees of freedom that the joint allocates including 3 translational movements in three-dimensional Cartesian coordinate and 3 rotational movements.

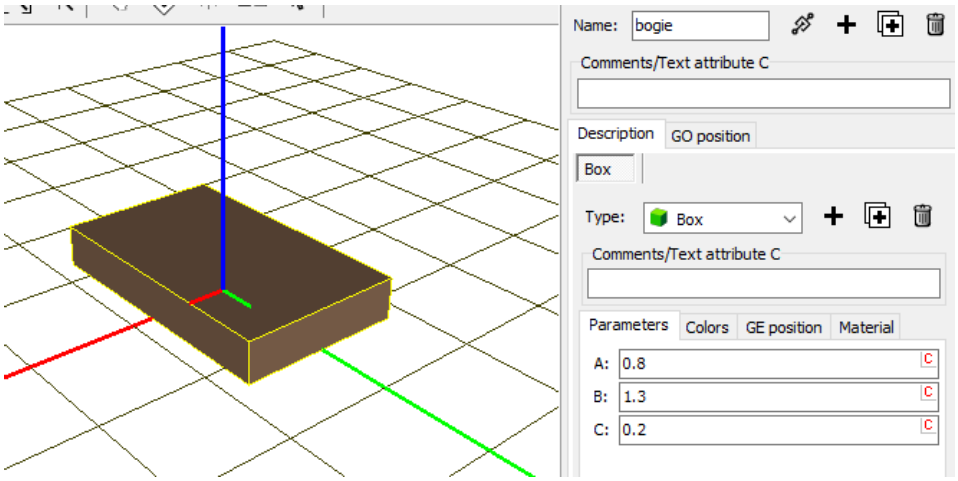

Figure 22. Parameter of bogie as image.

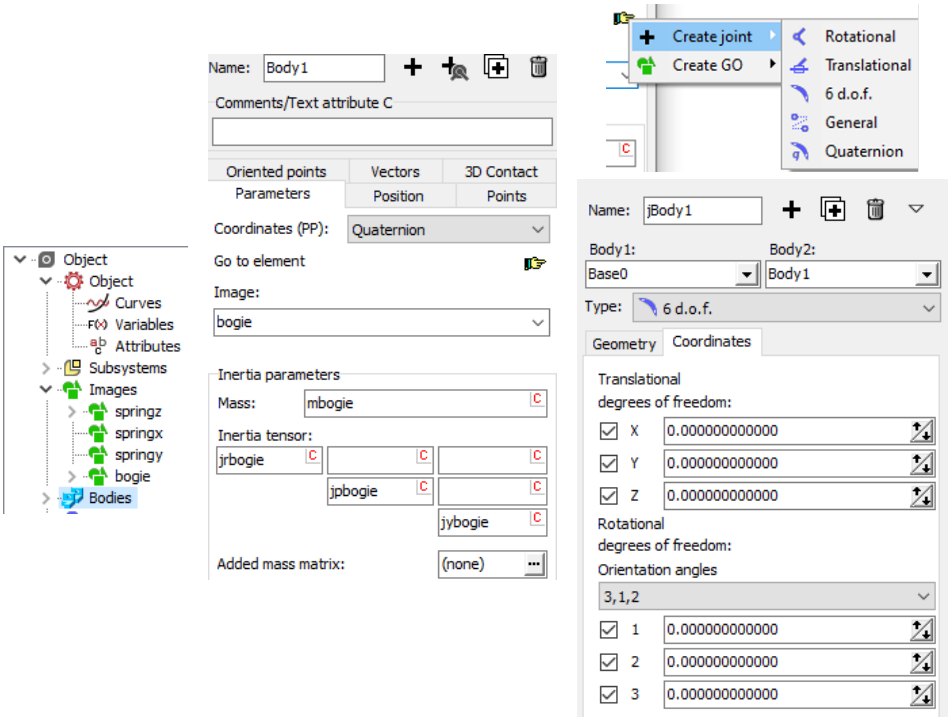

(a) (b)

Figure 23. Creating bogie as body, modifying its parameter (a), and creating joint for bogie (b).

3.9.4 Bipolar force element

A bipolar force element consists of a force between two fixed points in a line. The force may depend on distance, time, or time derivative of distance. Bipolar force is chosen to describe the spring and damper forces in this thesis. Below are paths to create spring elements in vertical direction:

1. Object > Bipolar forces > Add new element > Type > Linear

   A linear type bipolar force is created and shown in Figure 24. The spring force element is represented by the GO image of spring. Rename the force as springZ1L.

2. Object > Bipolar forces > springZ1L > Attachment points

   The force of springZ1L acts between the front left wheelset and Bogie. Attachment points are set and shown in Figure 25. The parameter $coordinate\ X0$ means the default length of the spring. It is calculated as:

$$X0 = h2 - h1 + fst1 \tag{3}$$

where $h1$ is the height of primary spring, $h2$ is the height of the bogie frame end. The $fst1$ equals the compressed length of the spring so that the springs can support their loads and keep other components stay at right places in the equilibrium state, in this case the load is the mass of bogie. The $fst1$ is calculated as:

$$fst1 = \frac{mbody + mbogie}{9.81 \cdot 4 \cdot c1z} \tag{4}$$

where $mbody$ is the mass of vehicle body. The $mbogie$ is total mass of all bogies. The number 4 is the quantity of springs. The $c1z$ is vertical stiffness of spring. After that, copy the force springZ1L 3 times, edit both acting body and attachment points according to Manchester Benchmark vehicle. All 4 springs in vertical direction are built.

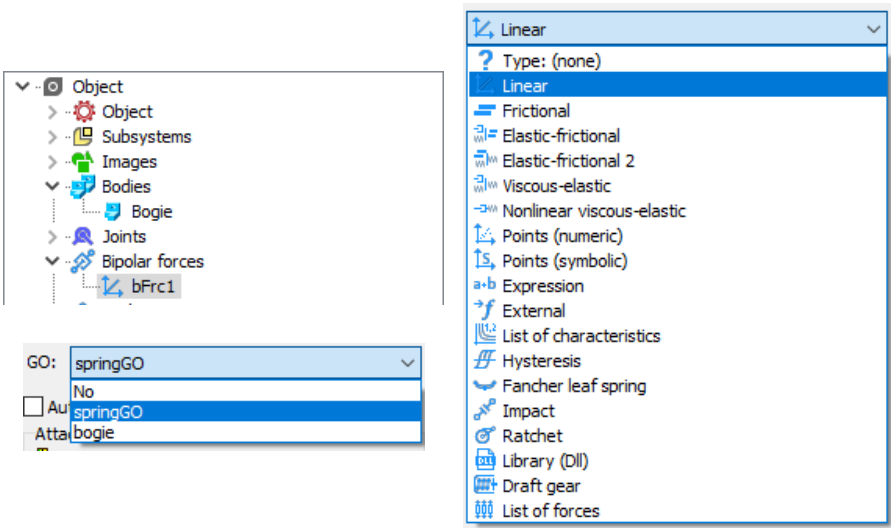

Figure 24. Creating bipolar force element.

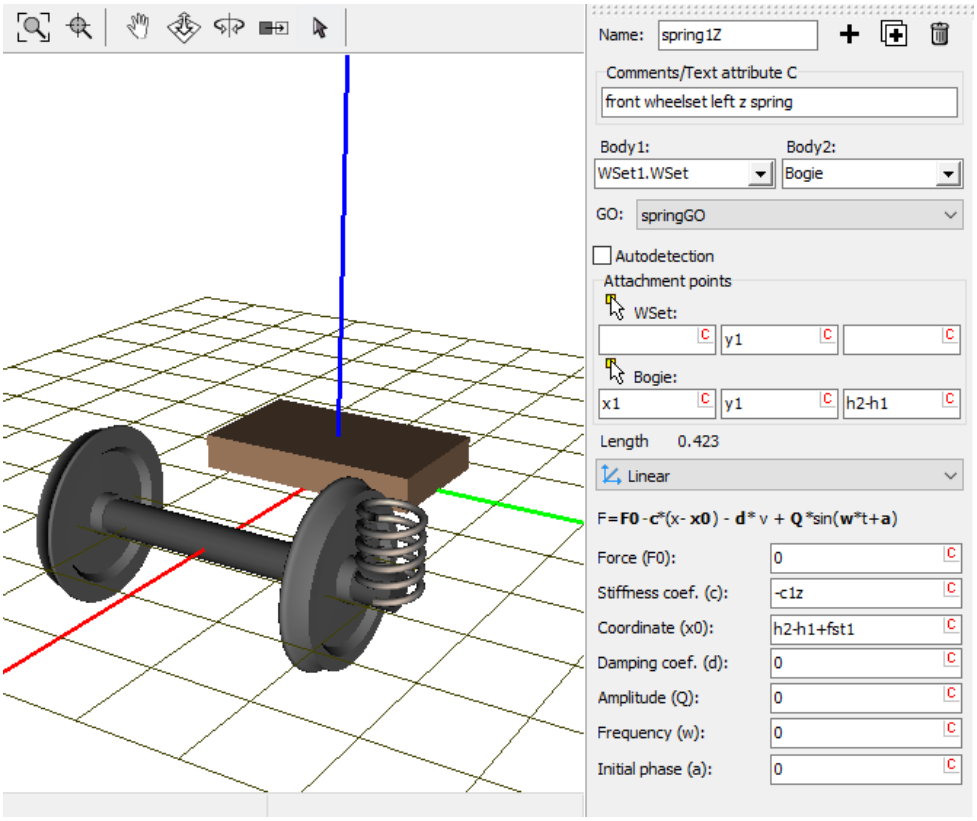

Figure 25. Attachment points and parameter of spring1Z.

3.9.5 Adding damper to vertical direction

A Viscous-elastic type of bipolar force is created and shown in Figure 26. Viscous-elastic element includes a linear spring, a parallel connection of spring and damper. In this case the parallel spring constant $c1 = 0$, the linear spring only connects with a damper in series. The spring constant in series $c1SeriesZ = 1 \times 10^6$ N/m, coefficient of linear dissipation $d1z = 4000$ Ns/m.

3.9.6 An example of spring and damper force in the longitudinal direction

The spring is created in the same way above. As it showed in Figure 27, the type is chosen as Expression so that both spring force and damper force can be included. The force expression that integrates spring and damper in longitudinal direction is expressed as:

$$F = -c1x \cdot (x - x1 + x2) - d1x \cdot v \tag{5}$$

where $c1x$ is longitudinal stiffness, x is real-time length of the spring, $x1$ is wheelset end semi-spacing, $x2$ is the bogie frame end semi-spacing, $d1x$ is nominal damping in parallel of longitudinal stiffness, v is vehicle speed.

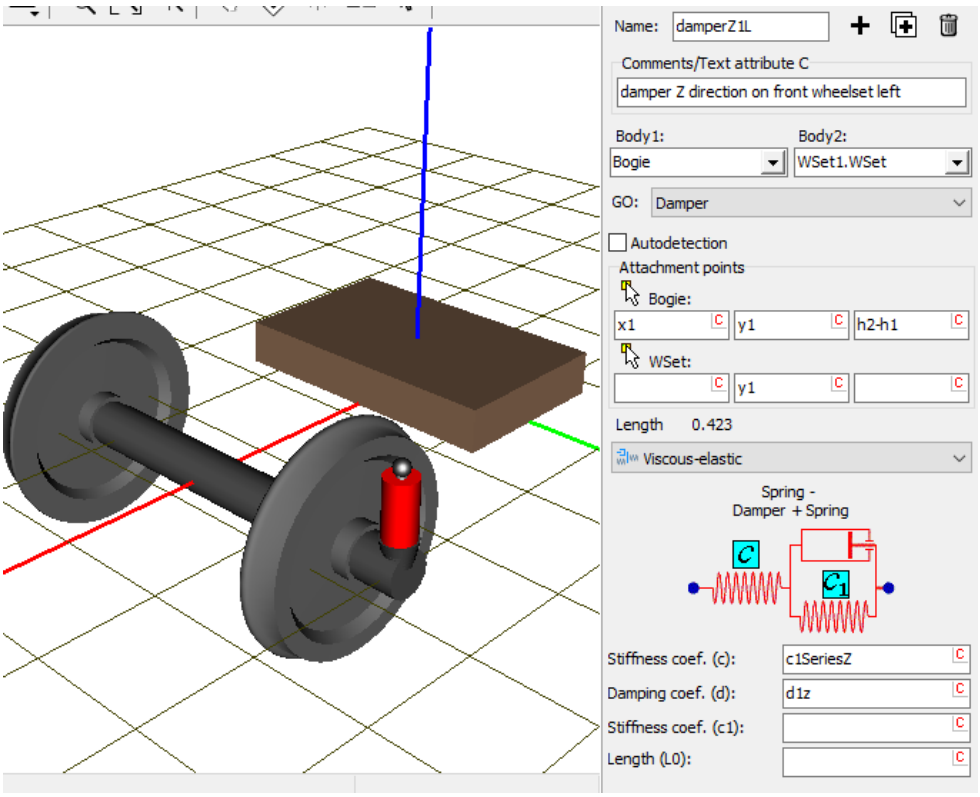

Figure 26. Damper in vertical direction on front wheelset.

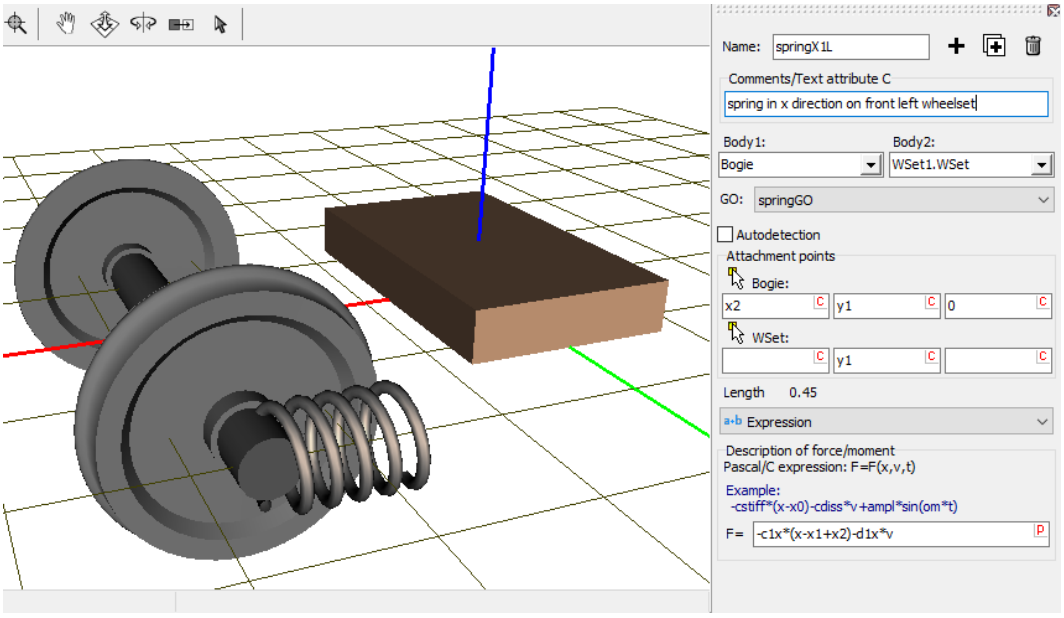

Figure 27. Spring and damper force expression in longitudinal direction.

3.9.7 Example of spring and damper force in lateral direction

As Figure 28 shows, the force of spring and damper in lateral direction are created in the same way as springX1L. The expression of the force is:

$$F = -c1y \cdot (x - y1 + y2) - d1y \cdot v \tag{6}$$

where $c1y$ is lateral stiffness, x is real-time length of the spring, $y1$ is wheelset end semi-spacing in the lateral direction, $y2$ is bogie frame end semi-spacing in the lateral direction, $d1y$ is nominal damping in parallel of lateral stiffness, v is vehicle speed.

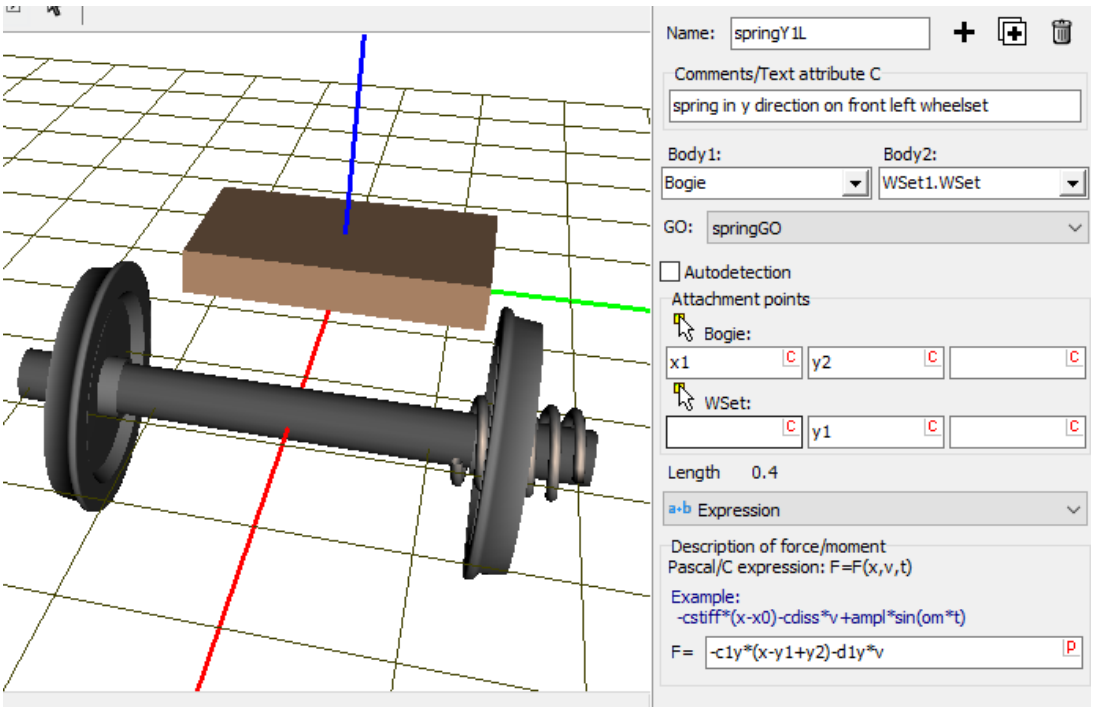

Figure 28. Settings of spring and damper in lateral direction between front wheelset and bogie.

4 NUMERICAL RESULTS AND ANALYSIS

The simulation results of one wheelset and Manchester Benchmark vehicle are introduced in this chapter. Figure 29 shows the two-point contact of the wheel rail profiles, which is appeared in both simulations. The important parameters of wheelsets are listed in Table 5. The R_0 is running circle radius. The α is conicity. Figure 30 shows ideal distance between the origin points of wheel frame and rail frame Δy. Δy can be expressed as (Simulation of Rail Vehicle Dynamics User's manual):

$$\Delta y = \frac{L_r - L}{2} \tag{7}$$

where L_r is the distance between centers of rail heads, L is the distance of wheelset running circles on left and right rail.

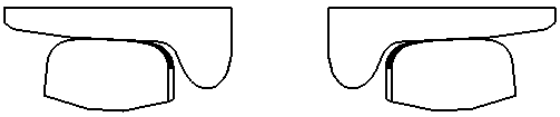

Figure 29. Benchmark wheel rail profile with two-point contact.

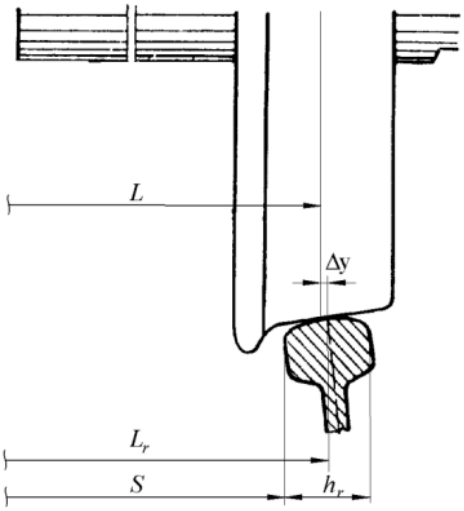

Figure 30. Benchmark wheel rail distance (Simulation of Rail Vehicle Dynamics User's manual).

Table 5. *Parameter of Benchmark wheel rail profile with two-point contact.*

Parameter	L (m)	R_0 (m)	L_r (m)	α (rad)
Value	0.7515	0.457	0.7555	1/40

Track irregularities are formed by spectral density functions (PSD) (Claus and Schiehlen, 1998). Points are pasted to UM irregularity editor to generate the irregularities related to both left and right rails. The irregularities of left and right lateral, left and right vertical are shown accordingly in Figure 31.

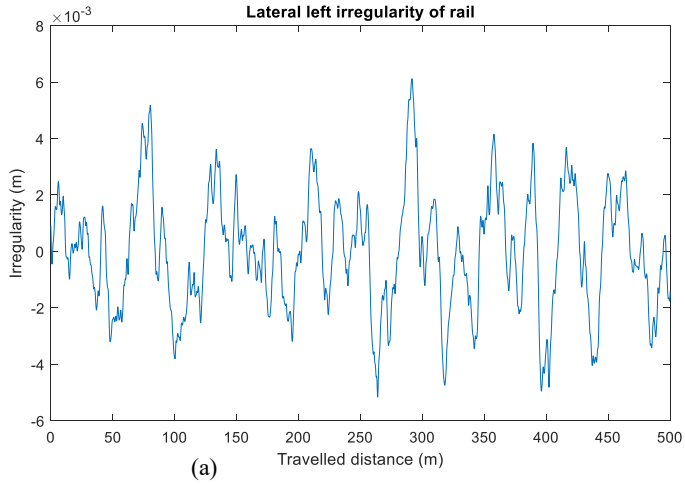

(a)

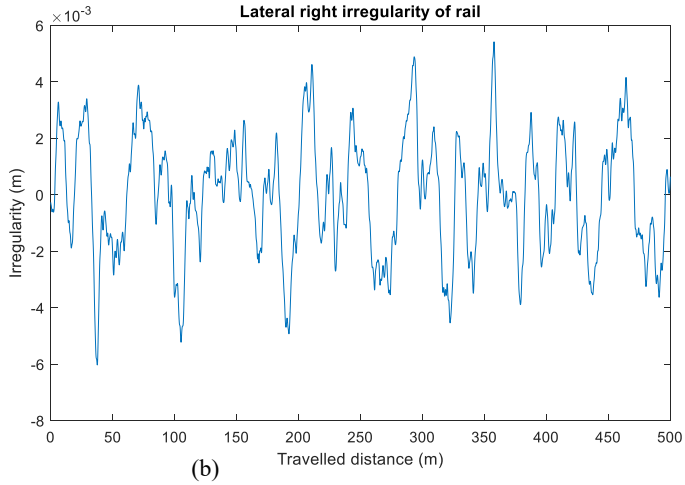

(b)

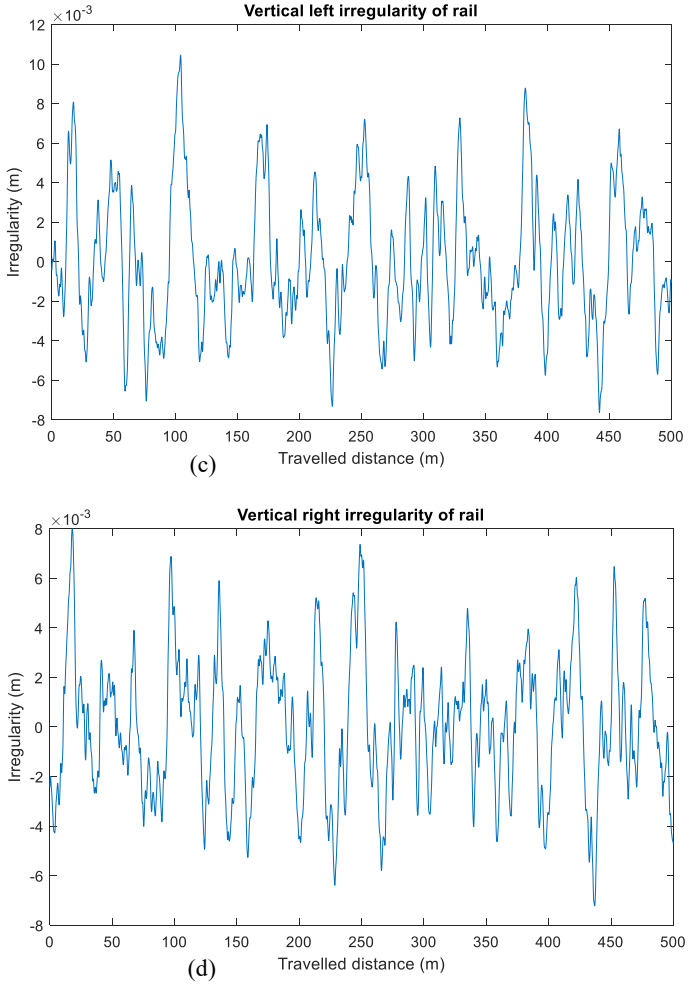

Figure 31. Irregularities of (a) lateral left, (b) lateral right, (c) vertical left, and (d) vertical right.

4.1 Klingel's frequency analysis of unsuspended wheelset on tangent track

Results of one wheelset forward motion on a tangent track are shown in Figure 32, Figure 33 and Figure 34. Wheelset with the constant forward speeds of 15 m/s, 25 m/s, and 45 m/s accordingly. Numerical results from UM and the lookup table method (Escalona, et al., 2019) are compared. 16.672 s is used for the 10 s simulation. Step size is 0.01. Results from UM agree well with MATLAB.

X coordinates are time, Y coordinates are lateral displacements of wheelset respected to the projection on track. Results from UM are shown in continuous line. Results from lookup table method is shown in dotted line.

Motion of one wheelset is unstable laterally because the wheelset is unsuspended. The initial lateral position is 3 mm. As the speed of wheelset grows, the cycle time is getting shorter and the wheelset is getting more and more unstable. The frequencies of 3 simulations obey Klingel's formula which is for the frequency of the small-scale kinematic oscillations of wheelset (Antali, et al., 2015):

$$\omega = V\sqrt{\frac{\alpha}{L_w R_0}} \tag{8}$$

where α is conicity of wheels as shown in Figure 8, L_w is the distance from wheel center to wheelset center, R_0 is the running cycle radius of the wheels when wheelset is centered on the track. For example, as it showed in Figure 32, forward velocity $\mathrm{V} = 15\ \mathrm{m/s}$, $\omega = 15 \times \sqrt{\frac{0.025}{0.75\times0.457}} = 4.05$ and $\mathrm{T} = \frac{2\pi}{\omega} = 1.55$ s. Frequency calculated by Klingel's formula is equal to the frequency of results from UM and Lookup table.

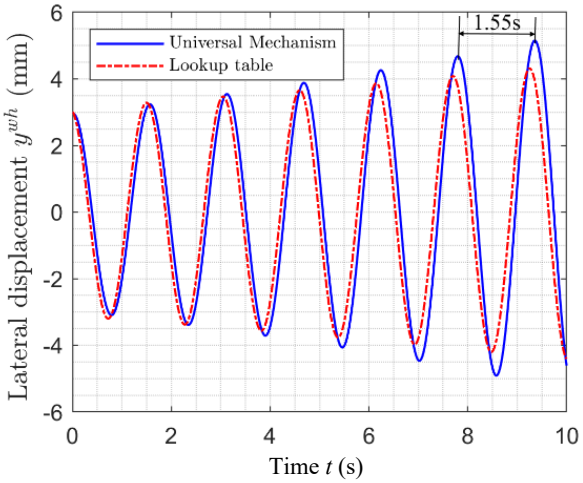

Figure 32. Comparation of y^{wh} between UM and Lookup table with forward velocity 15 m/s.

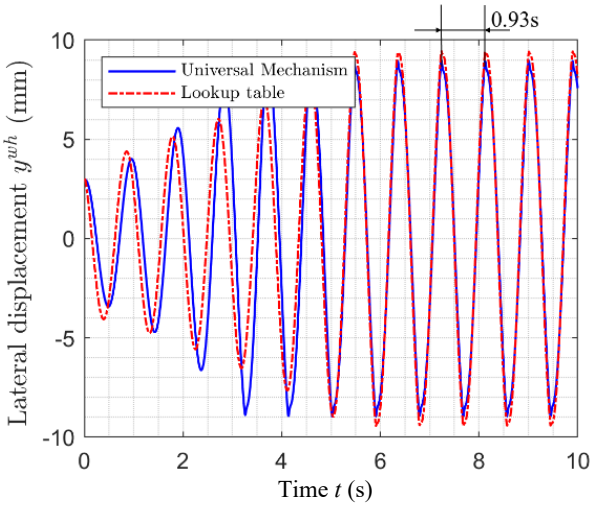

Figure 33. Comparation of y^{wh} between UM and Lookup table with forward velocity 25 m/s.

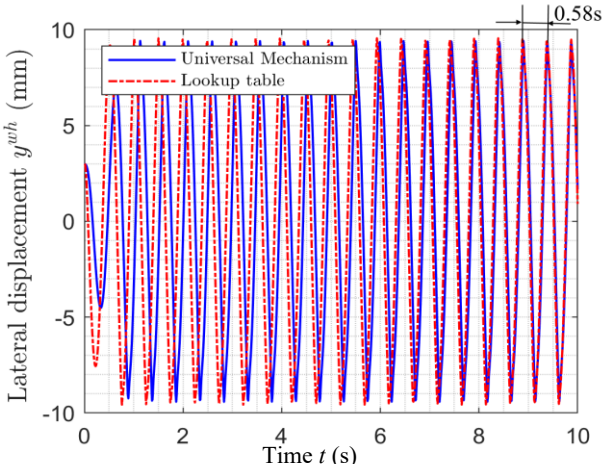

Figure 34. Comparation of y^{wh} UM and Lookup table with forward velocity 45m/s.

4.2 Stability analysis of unsuspended wheelset on a constant curvature track

This section presents the stability analysis of an unsuspended wheelset on different constant curvature tracks as shown in Figure 35 and Figure 36. Figure 37 is the comparison of wheelset lateral displacement in a steady curving large radius curve (R= 4545 m) between UM and Lookup table. Forward velocity is 20 m/s. The hunting is unstable. Symmetry axis y_{std}^{wh} of oscillation follows equation (Escalona, et al., 2012):

$$y_{std}^{wh} = -\frac{L_w R_0}{\alpha R} \tag{9}$$

where R is the radius of the curve. As shown in Figure 37, on large radius part, the oscillation is symmetry around -3 mm, which obeys $y_{std}^{wh} = -\frac{0.75\times0.457}{0.025\times4545} = -0.003\,m$.

Figure 38 shows comparation of wheelset lateral displacement on the general track with the small radius curve. $y_{std}^{wh} = -\frac{0.75\times0.457}{0.025\times235} = -0.058\,m$, the absolute value of y_{std}^{wh} is larger than the maximum lateral displacement $y_{max}^{wh} = 0.01\,m$. y^{wh} is constant when wheelset passing through the small radius curve, as stable curve negotiation with flange contact.

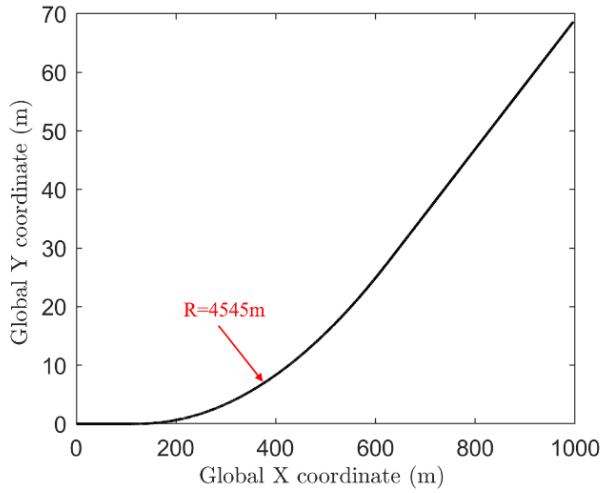

Figure 35. General track with large radius curve.

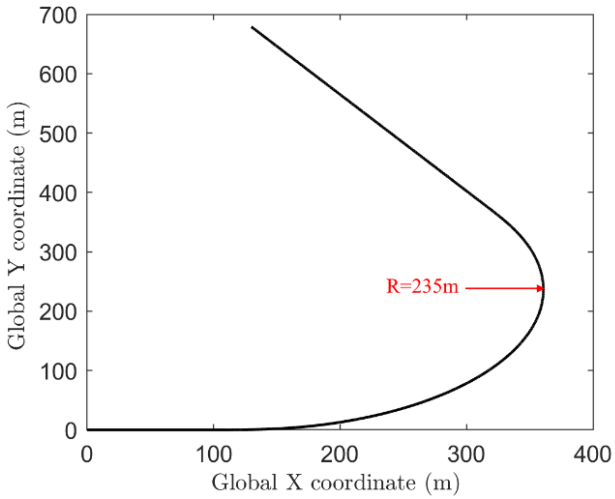

Figure 36. General track with small radius curve.

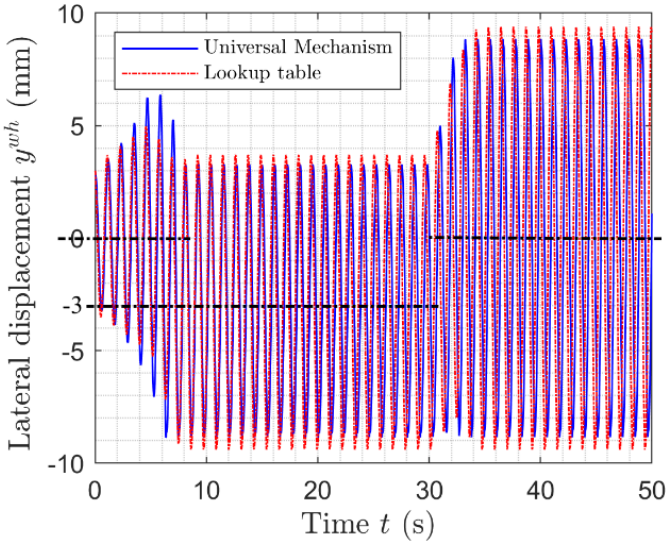

Figure 37. Lateral displacement of wheelset running on steady curving large radius curve track.

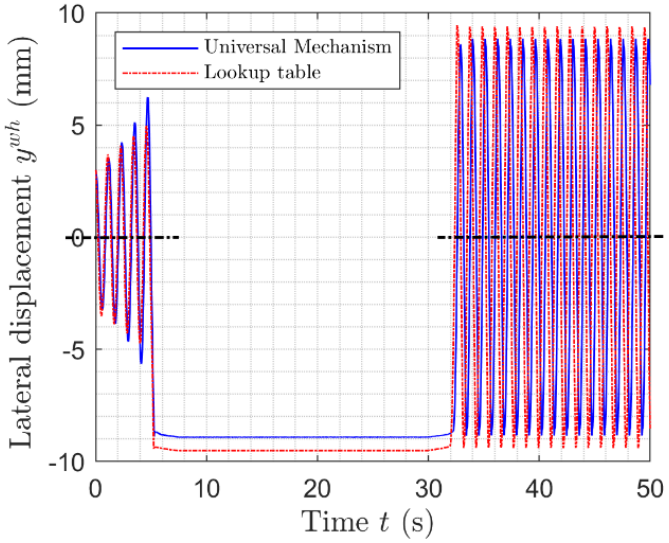

Figure 38. Lateral displacement of wheelset running on steady curving small radius curve track.

4.3 Manchester Benchmark

As it showed in Figure 39, the Manchester benchmark wagon is used. The center of rear bogie (right side) is chosen as the zero point when measuring the vehicle travelled distance. To compare the results between lookup table method, KEC method and UM, curved tracks

are used in simulations. Kinematics comparison results are shown in Figure 40, Figure 41, Figure 42, Figure 43.

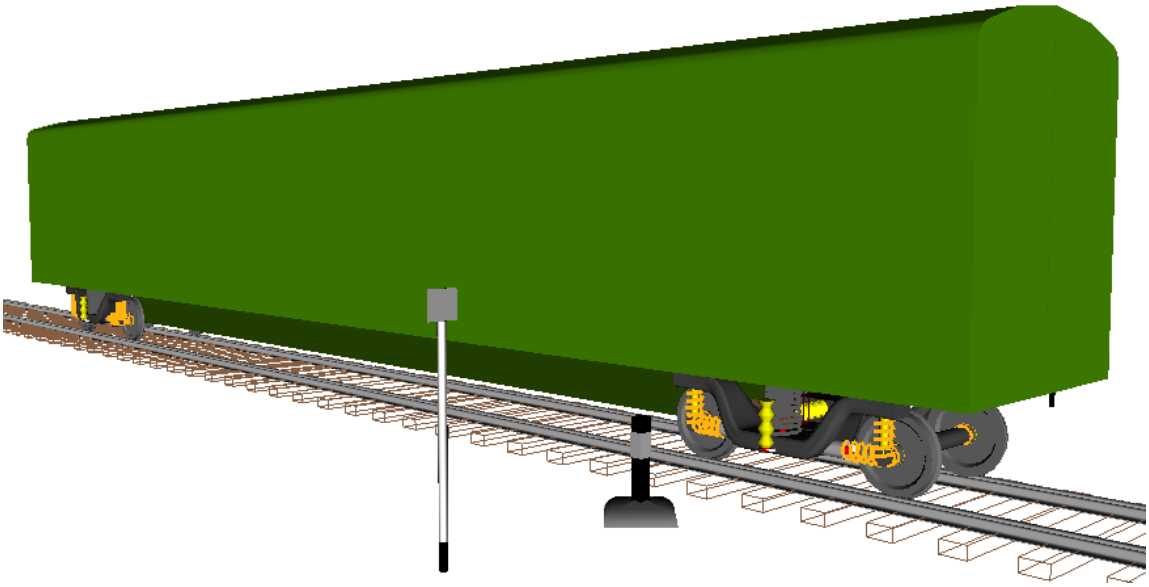

Figure 39. Manchester Benchmark wagon in UM.

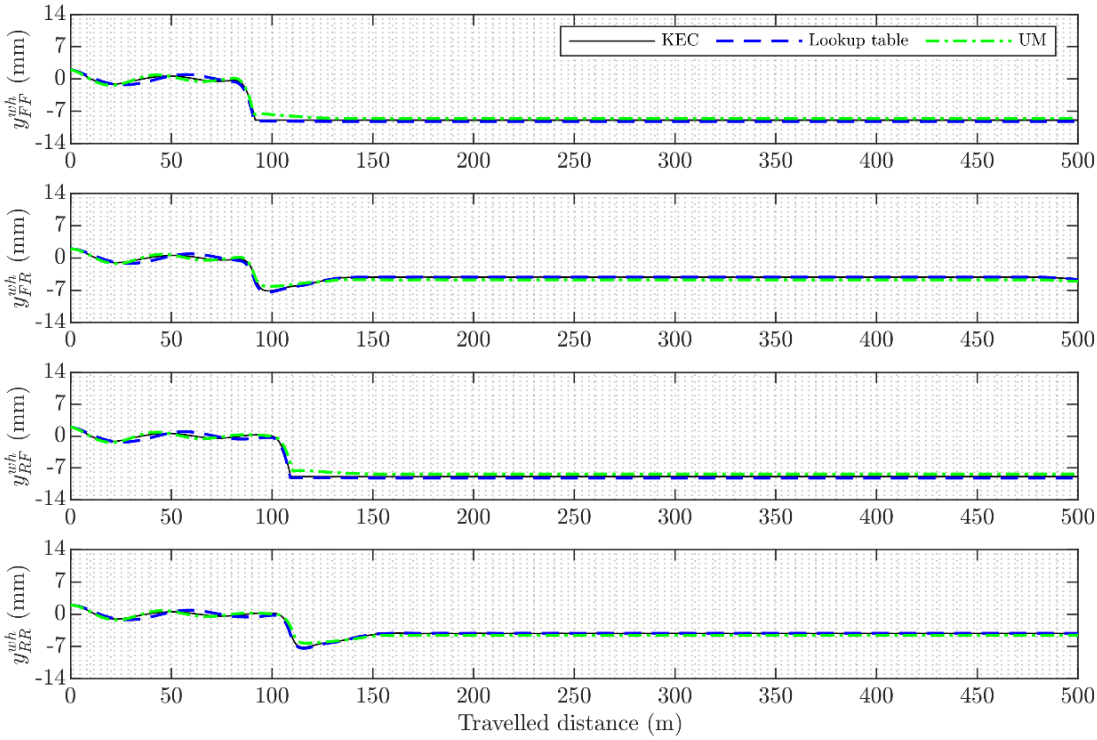

Figure 40. Comparison of lateral displacements of four wheelsets traveling on R=500 m even track.

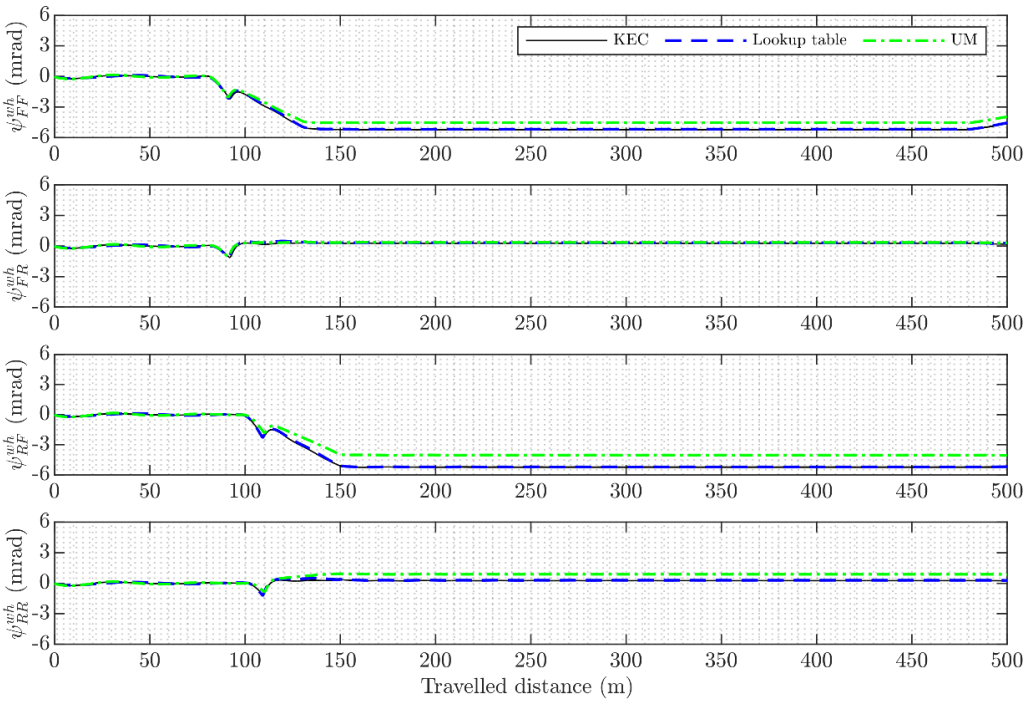

Figure 41. Comparison of yaw angles of four wheelsets traveling on R=500 m even track.

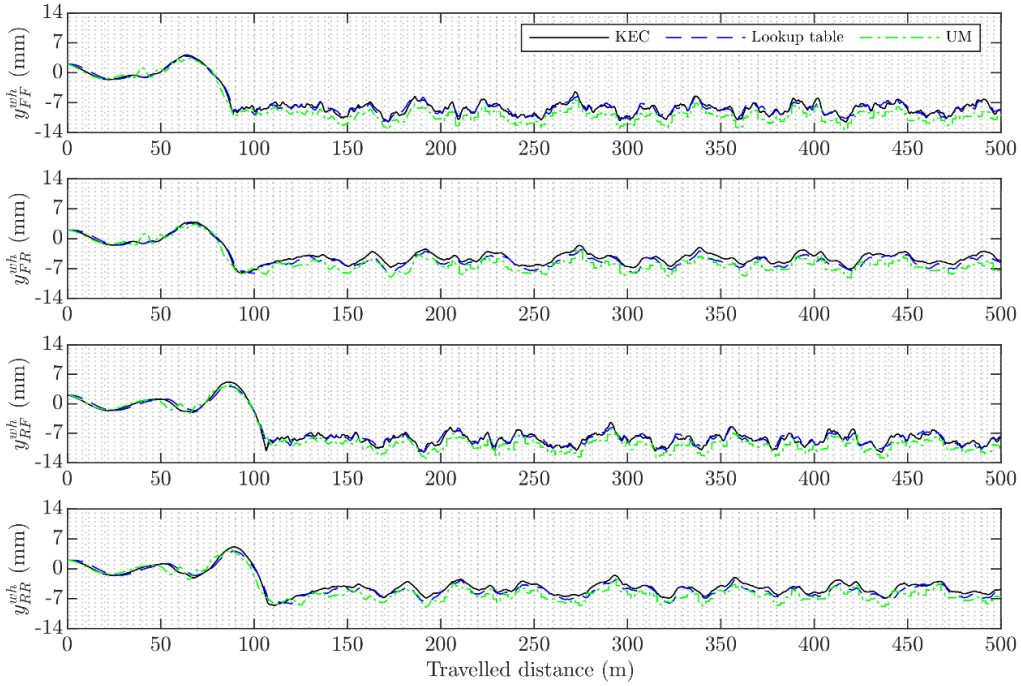

Figure 42. Comparison of lateral displacements of four wheelsets traveling on R=500 m track with irregularity

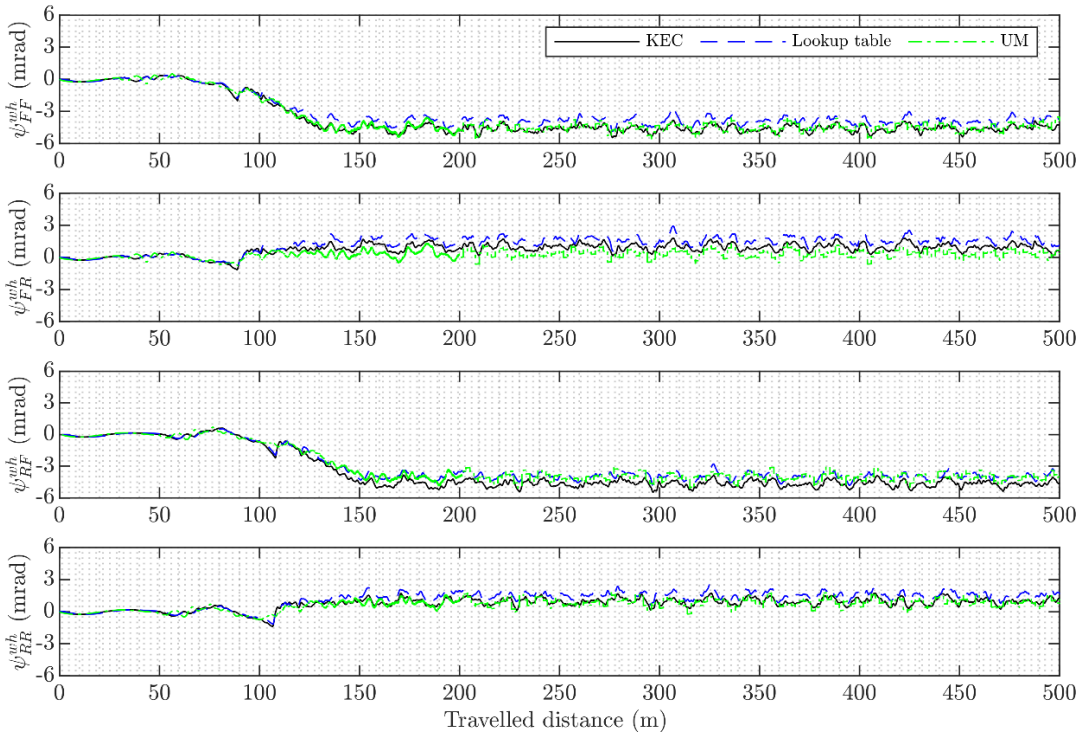

Figure 43. Comparison of yaw angles of four wheelsets traveling on R=500 m track with irregularity

The benchmark vehicle is simulated on 500-meter-long tracks with forward velocity 20 m/s. An even track is applied during the first journey. Irregularity of the track is applied during the second journey. The macro geometry of the track can be divided into three segments: 100-meter-long tangent part, 50-meter-long transition part, and 350-meter-long left curve track part with the radius of R=500 m. The results from the lookup table method, the KEC method and UM agree well with each other.

FF, FR, RF, RR are abbreviations of the front bogie front (wheelset), the front bogie rear (wheelset), the rear bogie front (wheelset), the rear bogie rear (wheelset) accordingly. The behavior of the lateral displacements of wheelset on the even track can be described separately to three sections below:

- When the vehicle travelling on the tangent section, the hunting starts from beginning because of the initial 2 mm of lateral displacement. Amplitude of hunting is decreasing because of suspension systems.

- When the vehicle travelling on the transition section, the hunting end. That is because the track is not tangential anymore.
- When the vehicle enters the steady curving section, the lateral displacements reach a constant value. It is steady because the flange contact appears, and the radius of the track is constant.

As mentioned before, the center of rear bogie is chosen as the zero point when measuring the travelled distance of the vehicle. The distance between rear and front bogies is 19 m. Front wheelsets start changing behaviors earlier than rear wheelsets. When the vehicle travels on the track with irregularity, the later displacement cannot reach a steady value because of the influence of irregularity.

5 CONCLUSION

This thesis introduced the background and advantage of railway vehicles. The railway transports of goods had a growing need during COVID-19 outbreak. Then it listed the objective of this work and introduced the structure of this thesis is introduced. The objective of the work is to evaluate the accuracy of the lookup table method (Escalona and Aceituno, 2019) and knife-edge-equivalent contact constraint (KEC) method (Escalona et al., 2019) which are implemented in MATLAB (by Xinxin Yu) in case of Manchester Benchmark parameters (Iwnick, 1998).

This thesis introduced theoretical foundations for the simulations: the rail wheel pairs, hunting, suspension systems, as well as cubic spline interpolation for profiles and irregularity. Then introduced integrators and the contact models of UM, GENSYS and VI-Rail. And then showed how to use the commercial software to build a bogie with primary suspension.

This study introduced the comparisons between the lookup table method, the KEC method and UM. The important contact parameters and the irregularities of the rails are emphasized firstly. The lookup table method, and the knife-edge-equivalent contact constraint method implemented in MATLAB in case of Manchester Benchmark are verified against Universal Mechanism. The lookup table method and the KEC method have good accuracy. The reason is that above two methods can get very close results with commercial software:

- For single wheelset travelling on a tangent track, lateral displacements from the lookup table method and Universal Mechanism are very close. The calculated Klingel frequency is the same as the frequency form simulation results.
- During the stability analysis of unsuspended wheelset on constant curvature tracks, the lateral displacements from the lookup table method and UM are also very close. The calculated result of symmetry axis on large radius curve track is the same as the axis measured from simulation result.
- For Manchester Benchmark vehicle simulation, lateral displacements, and yaw angles of four wheelsets are measured. The vehicle is simulated firstly on a small

radius (R=500 m) even track, and then on the same radius track but with irregularity accordingly. The results from above mentioned three methods are very close.

REFERENCES

Anon, (n.d.). Suspension Systems for Rolling Stocks. [online] Available at: http://www.railsystem.net/suspension-systems-for-rolling-stocks [Accessed 10 Nov. 2020].

Antali, M., Stepan, G. and Hogan, S.J., (2015). Kinematic oscillations of railway wheelsets. Multibody System Dynamics, 34(3), pp.259-274.

Barsky, B.A., (2013). Computer graphics and geometric modeling using Beta-splines. Springer.

Bertsekas, D.P., (2014). Constrained optimization and Lagrange multiplier methods. Academic press.

Claus, H. and Schiehlen, W. (1998). Modeling and simulation of railway bogie structural vibrations. Vehicle System Dynamics, 29(S1), pp.538–552.

Continental-railway.com. (2020). Continental railway - primary suspension. [online] Available at: https://continental-railway.com/en-gl/Bogie/Primary-Suspension [Accessed 10 Nov. 2020].

Deutsche Welle (www.dw.com (2018)). Trains vs. planes: What's the real cost of travel? | DW | 29.08.2018. [online] DW.COM. Available at: https://www.dw.com/en/trains-vs-planes-whats-the-real-cost-of-travel/a-45209552 [Accessed 29 Aug. 2020].

english.anhuinews.com. (n.d.). Railway freight between China and Finland hits record high-cnanhui.org. [online] Available at: http://english.anhuinews.com/system/2020/04/08/008395463.shtml [Accessed 6 Jul. 2020].

Escalona, J.L. and Aceituno, J.F. (2019). Multibody simulation of railway vehicles with contact lookup tables. International Journal of Mechanical Sciences, 155, pp.571–582.

Escalona, J.L., Aceituno, J.F., Urda, P. and Balling, O. (2019). Railway multibody simulation with the knife-edge-equivalent wheel–rail constraint equations. Multibody System Dynamics, 48(4), pp.373–402.

Escalona, J.L., Chamorro, R. and Recuero, A.M., (2012). Description of methods for the eigenvalue analysis of railroad vehicles including track flexibility. Journal of computational and nonlinear dynamics, 7(4). p. 041009

Gao, Y., Huang, H., Ho, C.L. and Hyslip, J.P., (2017). High speed railway track dynamic behavior near critical speed. Soil Dynamics and Earthquake Engineering, 101, pp.285-294.

Ibrahim, A., Abdullah, M.A. and Hudha, K., (2013). Multibody dynamics models of railway vehicle using Adams/Rail. Applied Mechanics and Materials, 393, pp.644–648.

Ingemar, P., (2020). Re: Ask about integration method and contact model of GENSYS [private e-mail]. Receiver: Dezhi Jiang. Sent 26.10.2020, 17:18 o'clock. (GMT +0200)

Iwnick, S., (1998). Manchester benchmarks for rail vehicle simulation. Vehicle System Dynamics, 30(3–4), pp.295–313.

Johnson, M.P., (2001). Environmental impacts of urban sprawl: a survey of the literature and proposed research agenda. Environment and Planning A: Economy and Space, 33(4), pp.717–735.

Kikuchi, N. and Oden, J.T., (1988). Contact problems in elasticity: a study of variational inequalities and finite element methods. Society for Industrial and Applied Mathematics.

Pombo, J.C.E.J. and Ambrósio, J., (2004). A multibody methodology for railway dynamics applications. Technical Report IDMEC/CPM-2004/003, IDMEC-Institute of Mechanical Engineering, Instituto Superi-or Técnico, Lisbon, Portugal.

Schorr, R. (n.d.). Vehicle-track modeling and simulation. [online] Available at: https://www.wheel-rail-seminars.com/archives/2018/pc-papers/presentations/PC07.pdf [Accessed 23 Oct. 2020].

Shabana, A.A. (2010). Computational dynamics. John Wiley & Sons, Ltd.

Shevtsov, I.Y., Markine, V.L. and Esveld, C., (2005). Optimal design of wheel profile for railway vehicles. Wear, 258(7-8), pp.1022-1030.

Simulation of rail vehicle dynamics user's manual. (n.d.). [online] Available at: http://www.universalmechanism.com/download/80/eng/08_um_loco.pdf [Accessed 29 Aug. 2020].

Sun, J., Chi, M., Cai, W. and Jin, X., (2019). Numerical investigation into the critical speed and frequency of the hunting motion in railway vehicle system. Mathematical Problems in Engineering, 2019.

TECHNIA. (n.d.). Simpack - fast non-linear multi-body simulations. [online] Available at: https://www.technia.com/software/simulia/simpack/ [Accessed 29 Aug. 2020].

Tiitu, M., (2018). Expansion of the built-up areas in Finnish city regions–the approach of travel-related urban zones. Applied Geography, 101, pp.1-13.

Um simulation program user's manual (2018). (n.d.). [online] Available at: http://www.universalmechanism.com/download/80/eng/04_um_simulation_program.pdf [Accessed 5 Nov. 2020].

Volker, B. (2020). Ask about VI rail integration method [private e-mail]. Receiver: Dezhi Jiang. Sent 26.10.2020, 11:50 o'clock. (GMT +0200). Attachment: 'virail.rar'.

Wriggers, P. and Zavarise, G., (2004). Computational contact mechanics. Encyclopedia of Computational Mechanics.

www.gensys.se. (n.d.). The CALC manual. [online] Available at: http://www.gensys.se/doc_html/calc.html#jtsim_param [Accessed 30 Oct. 2020].

www.universalmechanism.com. (n.d.). Universal Mechanism - the software for modeling of dynamics of mechanical systems: Home Page. [online] Available at: http://www.universalmechanism.com/cn/pages/index.php?id=1. [Accessed 29 Aug. 2020].

www.vttresearch.com. (n.d.). The SmartTram ecosystem brings attractive solutions to sustainable mobility while fostering competitiveness | VTT. [online] Available at: https://www.vttresearch.com/en/news-and-ideas/smarttram-ecosystem-brings-attractive-solutions-sustainable-mobility-while-fostering [Accessed 9 Nov. 2020].

www.xinhuanet.com. (n.d.). Xinhua Headlines: Railway freight express puts China-EU cooperation amid pandemic on fast track - Xinhua | English.news.cn. [online] Available at: http://www.xinhuanet.com/english/2020-06/27/c_139170811.htm [Accessed 6 Jul. 2020].

Table of contact models available in GENSYS (www.gensys.se)

p_lin	Defines a linear property
p_lin36	Defines a linear 6x6-matrix property
p_lin144	Defines a linear 12x12-matrix property
p_nlin	Defines a non-linear property
p_nlin_s	Defines an asymmetric non-linear property
p_nlin_t	Defines a non-linear property given by tangential values
p_nlin_st	Defines an asymmetric non-linear property given by tangential values
p_kfrkc	Property designed for coupling kfrkc
beam_1	Defines an Euler-Bernoulli beam connected to many masses
beam_3	Defines an Euler-Bernoulli beam with variable bending stiffness
c	Defines damper with a pre-defined property
c_l	Damper similar to c, oriented a small angle relative to esys
c_r	Damper similar to c, oriented a large angle relative to esys
c_vs_d	Defines a displacement-controlled damper
c12_b1	Defines a damping coupling between two masses of type m_rigid_12
c_magic_1	Defines a rolling contact between two masses according to the Magic Formula
creep_contact_1	Defines a rolling contact between two masses according to CONTACT
creep_contact_6	A wheel/rail-contact that utilizes the new features in CONTACT v18.1.5
creep_fasim_1	Defines a rolling contact between two masses. The normal contact is solved in a linear spring. The tangential contact is solved with Kalker's fasim routine.
creep_fasim_2	Similar to creep_fasim_1, but the creepages are modulated according formulas developed by: Maksym Spiryagin , Oldrich Polach & Colin Cole; Vehicle System Dynamics, 13 Aug 2013.
creep_fasim_4	Similar to creep_fasim_1, but this wheel/rail-coupling uses the wheel and rail profiles directly.
creep_lookuptable_1	Defines a rolling contact between two masses
creep_lookuptable_2	Defines a rolling contact between two masses
creep_polach_2	Defines a rolling contact between two masses. The normal contact is solved in a linear spring. The tangential contact is solved with O.Polach's ADH-routine.
creep_tanel_springs_1	Defines a rolling contact between two masses
coupler_1	Car-car coupler, buffer and/or draw-gear
coupler_2	Car-car coupler, buffer and/or draw-gear
derailm_2	Defines a contact element between two bodies
k, k_preZ	Defines stiffness with a pre-defined property
k_l, k_l_preZ	Similar to coupl k, but rotated a small angle relative to esys

k_r, k_r_preZ	Similar to coupl k, but rotated a large angle relative to esys
k12_b1	Defines a stiffness coupling between two masses of type m_rigid_12
k3, k3_preZ	Defines stiffness with 3 pre-defined properties
k3_l, k3_l_preZ	Similar to coupl k3, but rotated a small angle relative to esys
k3_r, k3_r_preZ	Similar to coupl k3, but rotated a large angle relative to esys
km, km_preZ	Similar to coupl k, but the user can control if the coupling shall generate moments on attached masses or not
km_l, km_l_preZ	Similar to coupl km, but rotated a small angle relative to esys
km_r, km_r_preZ	Similar to coupl km, but rotated a large angle relative to esys
k_air3	A coupling for modeling airbags in railway vehicles.
k_air3_exp	A coupling for modeling airbags in railway vehicles with exponential smooth friction in the horizontal plane.
k_air3_mawa	A coupling for modeling airbags in railway vehicles, using equations for viscous flow in pipes in vertical direction.
k_air3_mawa2	A coupling for modeling airbags as in coupling k_air3_mawa, but with two auxiliary air reservoirs in parallel.
k_coil3	A coupling for modeling of vertically standing coil springs.
kc	Defines a spring in series with a damper.
kckc	Defines a coupling consisting of two dampers and two springs. The first spring and damper are connected in parallel with each other
kf	Defines a friction block with series flexibility
kf_l	Similar to coupl kf, but rotated a small angle relative to esys
kf_r	Similar to coupl kf, but rotated a large angle relative to esys
kf2	Defines a two-dimensional friction block with two perpendicular serial flexibilities
kf2_l	Similar to coupl kf2, but rotated a small angle relative to esys
kf2_r	Similar to coupl kf2, but rotated a large angle relative to esys
kf3	Defines a three-dimensional friction block with three perpendicular serial flexibilities
kfrkc	Defines a coupling with smooth friction and viscous damping
kf_exp1	Defines a coupling comprising a stiffness with exponential friction
kf_exp2	A stiffness coupling with a exponential shaped friction added on
kf_exp3	A stiffness coupling with a smooth friction added on
m_flex_1	Links a coupling to a flexible body
m_flex_m6	Links a coupling to a flexible body with a moving attachment point
cuser#	Defines a coupling whose properties are defined in an own supplied subroutine CUSER# (# is a number between 0 and 9)